

CHARACTERIZATION AND ELIMINATION OF  
DEFECTS IN METALLIC GLASS HONEYCOMB

By

GANAPATHI RANJAN MAHADEVAN

Bachelor of Engineering in Mechanical Engineering

Visveswaraiah Technological University

Belgaum, Karnataka

2006

Submitted to the Faculty of the  
Graduate College of the  
Oklahoma State University  
in partial fulfillment of  
the requirements for  
the Degree of  
MASTER OF SCIENCE  
July, 2011

CHARACTERIZATION AND ELIMINATION OF  
DEFECTS IN METALLIC GLASS HONEYCOMB

Thesis Approved:

Dr. Jay C. Hanan

---

Thesis Advisor

Dr. Kaan Kalkan

---

Dr. Sandip P. Harimkar

---

Dr. Mark E. Payton

---

Dean of the Graduate College

## ACKNOWLEDGMENTS

First of all, I would like to thank my Advisor Dr. Jay Hanan for his guidance, support and advise, which have not only aided in helping me mature as a researcher but have also added an invaluable positive dimension to my overall personality. His ways of time management; and his keen foresight to accurately predict outcomes at the very beginning of every task made my work simpler than it would have been. These fine qualities apart, what I have always admired in Dr. Hanan are; the fairness with which he makes all his decisions and his forgiving nature. My utmost respect for him stems from these qualities. Without his support this project couldn't have been carried out.

I would like to convey my sincere thanks to Mike Lucas from the Department of Physical Sciences, for his invaluable inputs which were instrumental in designing the manufacturing technique for MG Honeycombs. During the course of designing a good technique for manufacturing MG honeycombs I have had to use the Design and Machining Laboratory (DML) extensively. I thank John Gage here for all the support he extended during the course of my work at DML.

I thank Dr. Kenneth Ede without whose help the study on cell wall defects couldn't have been completed successfully. He is one of the most down to earth people I have met. My many thanks to American Airlines Inc, Tulsa OK who were magnanimous to provide aluminum honeycombs for our research. My sincere thanks to Dr.Kaan Kalkan and Dr. Sandip Harimkar for agreeing to be on my committee in spite of their busy schedules.

I thank Balaji Jayakumar and Sudheer Bandla who trained me on the experimental methods and test equipment. Their guidance has proved invaluable in more ways than one. My sincere thanks to my group mates Masoud Allahkarami, Reajuddin Ahmed, Rohit Vaidya and Advait Bhat for their support during the course of this work. I would also like to thank Ashish and Mrinalini for all the good discussions that I have had with them on BMGs and for their support with my experiments.

I feel indebted to my friends Ajith, Akshata, Ashwin, Krishnan, Mithun, Muthappa, Praful, Rachana, Raghavendra, Rahul, Rajshekhar, Shridhar, Sonal and Sushil for the support that they extended through the course of my work here at OSU.

I cannot thank enough, my sister Deepa Mahadevan, my brother Sharath; back home in India, and my fiancé Aarthi Muralidhar for their patience and support. I am lost for words to express my gratitude to my parents, Lakshmi Mahadevan and Mahadevan .G without whose blessings I wouldn't have come this far.

## Table of Contents

1. INTRODUCTION .....	1
1.1. Stimulus.....	1
1.2. Synopsis.....	2
1.3. Prior Work.....	3
Honeycombs .....	3
Honeycomb manufacturing methods .....	4
Mechanical behavior of Cellular Structures .....	5
Effect of Defects on Honeycomb performance .....	8
Response of Honeycombs to Multi-axial and inclined loading .....	9
Metallic Glasses .....	12
Metallic Glass Honeycombs .....	13
2. MATERIALS and METHODS.....	17
2.1. Metallic Glass Ribbon-MetGlas 2826 MB.....	17
2.2. Continuous Ribbon Winding Method for manufacturing Tear Drop Lattice honeycombs.....	18
2.3. Properties of Adhesives used in manufacturing TD lattice honeycombs.....	22

Adhesive shear strength test.....	22
2.4. Quasi-Static Compression Testing of Honeycombs.....	23
Out of plane compression testing of Metallic Glass Honeycombs .....	23
In-plane compression testing of MG Honeycombs .....	24
Compression testing of Aluminum honeycombs .....	25
2.5. Comparison of Geometry of Old and New teardrop lattice Honeycombs using Micro Computed Tomography .....	25
2.6. Quasi-Static compression testing of honeycombs with inclined cell axis.....	26
Procedure .....	26
Sample preparation .....	28
3. RESULTS .....	30
3.1. Features of continuous ribbon winding method .....	30
3.2. Properties of Adhesives used in Tear Drop lattice honeycombs.....	31
3.3. Mechanical properties of Metallic glass honeycombs .....	32
Out of plane properties of Metallic Glass Honeycombs.....	32
In plane properties of Metallic Glass Honeycombs.....	35
3.4. Geometry comparison of folded and wound Metallic Glass honeycombs.....	36
3.5. Effect of cell axis inclination on Honeycomb performance .....	37

4.	Discussion .....	41
4.1.	Properties of Wound Metallic Glass Honeycombs .....	41
4.2.	Inclined Honeycomb Section tests .....	43
5.	Conclusions and Future recommendations .....	44
5.1.	Properties of defect free (Wound) MG Honeycombs .....	44
5.2.	Effect of Cell Axes Inclination or inclined loading on honeycomb strength .....	45
	REFERENCES .....	46
	APPENDICES .....	48
	Appendix I.....	48
	Design concepts for ribbon winding method of manufacturing Metallic Glass Honeycombs .....	48
	Appendix II.....	54
	Difficulties in machining expanded aluminum honeycombs.....	54

## LIST OF TABLES

Tables	Page
Table 2-1 Physical properties of MetGlas 2826 MB [31].....	17
Table 2-2 Specifications of Honeycombs tested.....	25
Table 2-3 Specifications of honeycomb used for making skewed sections...	27
Table 3-1 Peak Stress, Plateau stress, Young's modulus and Energy absorbed for each honeycomb .....	34
Table 3-2 Cell axis misorientation in folded and wound honeycombs.....	36

## LIST OF FIGURES

Figure	Page
Figure 1-1 Different honeycomb cell shapes.....	4
Figure 1-2 Honeycombs manufactured by crimping low density metal sheets and then resistance welded or adhesively bonded to form corrugated cores. ....	4
Figure 1-3 Honeycomb manufactured by expansion method. ....	5
Figure 1-4 Honeycomb principal directions. ....	6
Figure 1-5 Plot of honeycomb compression with multiple relative densities.....	6
Figure 1-6 Failure stress normalized by E. ....	7
Figure 1-7 Phases of honeycomb collapse under compressive loads. ....	8
Figure 1-8 Modified Arcan's apparatus used to apply inclined loads...	10
Figure 1-9 Results showing the decrease in peak strength of aluminum honeycombs with increasing load inclinations. ....	10
Figure 1-10 Normal Stacking pattern (Left) and inclined stacking pattern (Right) in honeycombs.....	11

Figure 1-11 Resilience $\sigma_2 y / E$ plotted against loss co-efficient $\eta$ for 1507 metals, alloys, metal matrix composites and metallic glasses. ....	13
Figure 1-12 Armor panel with Tear Drop lattice core which successfully stopped four bullets .....	14
Figure 1-13 Track and slider used for making TD lattice rows. ....	15
Figure 1-14 Tear Drop lattice ribbon formed by using the width of the ribbons as the height. ....	15
Figure 1-15 Non-uniformity in cell shape and size seen in a small Folded Tear-Drop Lattice sample. ....	16
Figure 1-16 Pronounced Cell height misalignment in Folded Metallic Glass Honeycombs .....	16
Figure 2-1 Fe <sub>45</sub> Ni <sub>45</sub> Mo <sub>7</sub> B <sub>3</sub> - MetGlas 2826 MB. ....	17
Figure 2-2 Ribbon wound around dowel pins.....	18
Figure 2-3 A long tear-drop lattice row on application of adhesive. ....	19
Figure 2-4 (a) and (b) Base plate inverted; cells' faces flush with flat surface.....	19
Figure 2-5 A 820 mm <sup>2</sup> TD lattice sample. ....	20
Figure 2-6 A 5 in x 3 in Metallic Glass honeycomb plate. ....	21
Figure 2-7 A schematic representation of Lap jointed ribbon specimens.....	22
Figure 2-8 Super glue lap joint shear strength test. ....	23

Figure 2-9 Tear Drop Lattice Honeycomb under quasi-static compression between two platens.....	24
Figure 2-10 A front view of reconstructed radiographs (a) folded sample (b) wound honeycomb samples.....	26
Figure 2-11 Skewed aluminum honeycomb section.....	27
Figure 2-12 Honeycomb section mounted at fifteen degrees on a cut-off-saw.....	28
Figure 2-13 Precision angle block used to set the vise jaw angle.....	29
Figure 2-14 Honeycomb with inclined cell axes.....	29
Figure 3-1 Comparison of apparent shear strength of Cyanoacrylate gel and Multi temperature hot melt.....	31
Figure 3-2 Stress-Strain plot comparing MG honeycombs to aluminum honeycomb.....	32
Figure 3-3 Random collapse pattern and extensive bond failure in MG honeycombs.....	33
Figure 3-4 Regular stacking pattern seen in crushed aluminum honeycombs .....	33
Figure 3-5 Stress-strain curves for Metallic Glass Honeycombs indicating the irregular plateau .....	34
Figure 3-6 Stress-Strain data for wound MG Honeycombs along in-plane directions .....	35

Figure 3-7 Stress-strain curves for folded MG honeycombs along the in-plane directions [2].	35
Figure 3-8 Plots for (a) $90^\circ(X_3)$ and $87^\circ$ sections (b) $85^\circ$ and $83^\circ$ (Steep Drop in plateau stress)	38
Figure 3-9 Plots for (a) $80^\circ$ and $75^\circ$ sections (b) $72.5^\circ$ and $71.5^\circ$ (Steep Drop in plateau stress)	38
Figure 3-10 Plots for (a) $70^\circ$ , $65^\circ$ and $60^\circ$ sections (b) $60^\circ$ and $0^\circ$ ( $X_1$ )	39
Figure 3-11 Stress-strain plot for all skewed sections	39
Figure 3-12 Plot of (a) Crush stress Vs. Cell axes inclination (b) Young's modulus vs. Cell axes Inclination.	40

## CHAPTER I

### 1. INTRODUCTION

#### 1.1. Stimulus

This work is a part of the ongoing research on the Metallic Glass Teardrop lattice Honeycomb which was recently developed, in 2009, by Jay C. Hanan and Balaji Jayakumar [1]. There are no exact analytical models that predict the properties of Teardrop lattices. Ashby's model which serves as a fair start, predicts a very high yield strength of 25.4MPa. However, experiments yielded a significantly lesser value of 3.4 MPa. This was attributed to defects such as cell wall misalignment, cell wall disorientation, and non-uniform cell size; inherent to the manual method of manufacturing. The following objectives were proposed as future work:

1. Eliminating defects by devising a new method of manufacturing and characterizing the mechanical properties of the honeycombs.
2. Understanding the strain rate response of metallic glass honeycomb.
3. Identifying the contribution of adhesives to the strength of metallic glass honeycomb.

With respect to the first objective it was identified that eliminating cell axis misorientation would contribute greatly to honeycomb strength

Therefore, it was important to identify the effect of normal loads on honeycombs with cell axial misorientation. Furthermore, metallic glass honeycomb was basically developed as an energy absorber in body armors. In context, the loading during ballistic impact is never in line with the cell axis. Therefore, the impact of oblique loads on honeycombs needed study. In summary, the study of oblique loading on honeycombs along with the proposed objectives in [2] serves as the stimulus for the present work.

## **1.2. Synopsis**

A new lab scale method of manufacturing has been devised to produce defect free metallic glass honeycombs. This method has reduced cell wall misorientation from  $15^\circ$  to  $1.5^\circ$  and yielded more uniform cell geometry. A threefold improvement in the strength of teardrop lattice honeycombs was observed with the use of this new manufacturing method.

Metallic glass honeycomb (MGH) manufactured using the new method, henceforth addressed as wound MGH (or wound tear drop honeycomb) has been compared with conventional Aluminum 5052 honeycomb of an equivalent areal density and was found to exhibit 15% higher yield strength. This is substantial considering that the product is in its developmental stages.

As a step towards investigating the effect of adhesives on the strength of teardrop lattice honeycombs, samples prepared using two different adhesives, Cyano-Acrylate Adhesive and the previously used Hot-Melt were compared. To understand the effect of cell axis misorientation on honeycomb strength, off-axis (specimens with an inclined cell axis) aluminum honeycomb sections were tested under normal loading conditions. This

not only assists in understanding the importance of cell axis geometry but also aids in perceiving the effect of oblique loads on honeycombs.

Results of all experiments carried out on the wound tear drop Honeycombs have been presented in the following sections and further improvements have been recommended to bring out the full potential of these honeycombs.

### **1.3. Prior Work**

#### **Honeycombs**

Honeycombs are made up of an array of prismatic cells which nest together to fill a plane [3]. Due to their low stiffness to weight ratio and mechanical energy absorbing characteristics, their range of applications as structural materials is pervasive. Their high strength to weight ratio has gained them extensive usage in the aircraft industry as composite cores which make up the control surfaces such as wings, slats, and ailerons. They are also used widely as crash barriers for efficient impact energy absorption in the automotive industry [4].

Honeycombs are manufactured out of a wide variety of materials like paper, metal, and phenolic resin. Of all honeycombs, aluminum honeycombs are the most widely used. There are different types of honeycombs based on cell shape and size to suit various applications (Figure 1-1). In 2009 Jay C. Hanan and Balaji Jayakumar [2] developed a new class of honeycombs using metallic glass ribbons with the cell shape in the form of a teardrop, continuation of which is in the subject of this thesis.

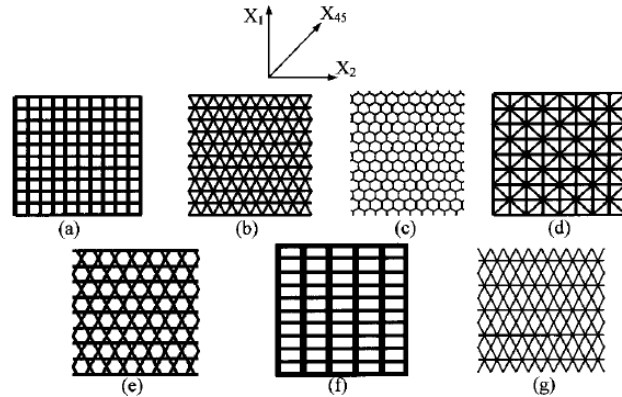


Figure 1-1 Different honeycomb cell shapes [5].

### Honeycomb manufacturing methods

Wadley and Affleck *et al.* 2003 [6] have described: various methods of manufacturing, different base materials, and novel techniques and tools to fabricate honeycombs of various cell shapes and sizes. Wadley *et al.* [6]; and Burton and Noor [7] analyzed the various types of bonding and related variables in Honeycombs. The two methods of manufacturing honeycombs-bonding corrugated strips and expansion method-are shown in Figure 1-2 and Figure 1-3.

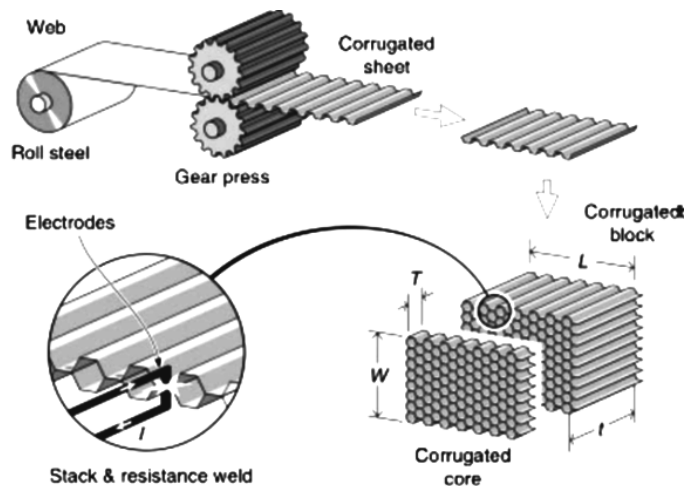


Figure 1-2 Honeycombs manufactured by crimping low density metal sheets and then resistance welded or adhesively bonded to form corrugated cores [6].

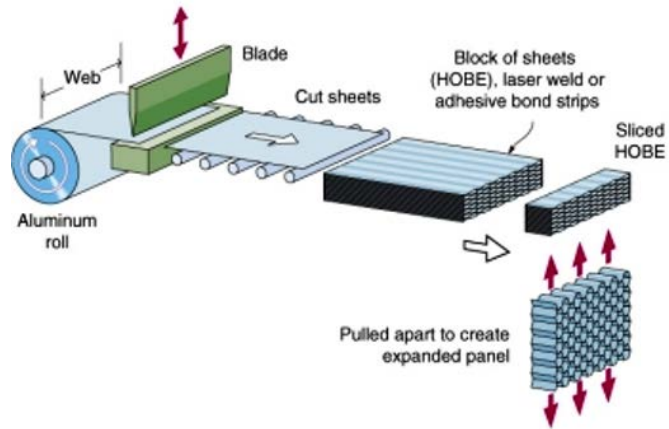
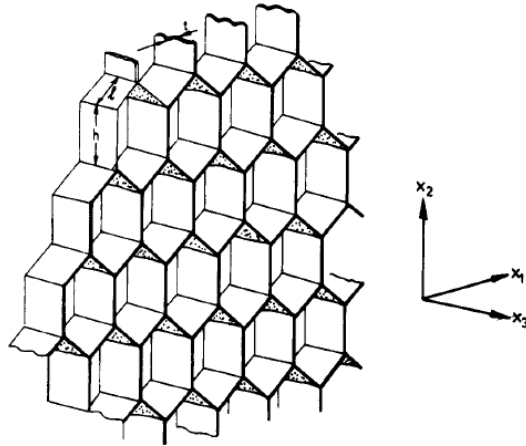


Figure 1-3 Honeycomb manufactured by expansion method [8].

### Mechanical behavior of Cellular Structures

Honeycombs are anisotropic and exhibit maximum strength along the out-of-plane direction; also referred to as the  $X_3$  direction or the load bearing direction. The principal directions in a honeycomb are shown in Figure 1-4. Honeycombs are usually described by their  $t/l$  (cell wall thickness to length) ratio and relative density. The range of cell wall thicknesses for honeycombs is 50-100 microns [9], and the lower limit for the ratio of the cell wall thickness to length ( $t/l$  ratio) is 0.1. The relative density is the most important parameter used to describe cellular structures and is usually in the range of 0.1-0.3 [9].



**Figure 1-4 Honeycomb principal directions [3].**

The bulk properties of honeycombs such as yield strength, Young's modulus, crush strength, and densification strains are usually obtained through compression and shear tests. The mechanical properties of honeycombs in both in-plane and out of plane directions have been investigated thoroughly by many researchers. The out of plane properties have been studied under both compressive and shear loading, and analytical models have been derived [4, 10]. Zhang and Ashby [10] showed that the density of honeycombs acutely influence their out of plane behavior (Figure 1-5 and Figure 1-6).

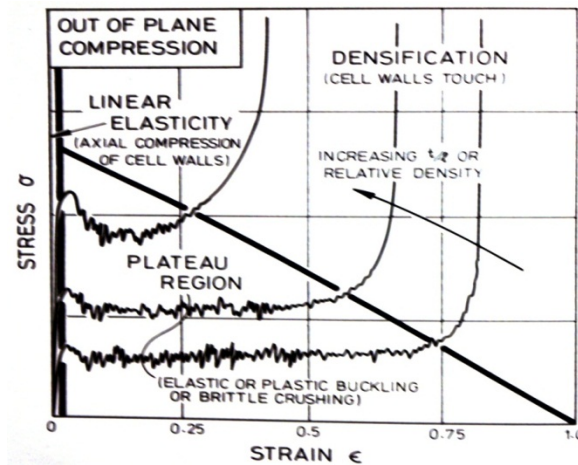


**Figure 1-5 Plot of honeycomb compression with multiple relative densities [3].**

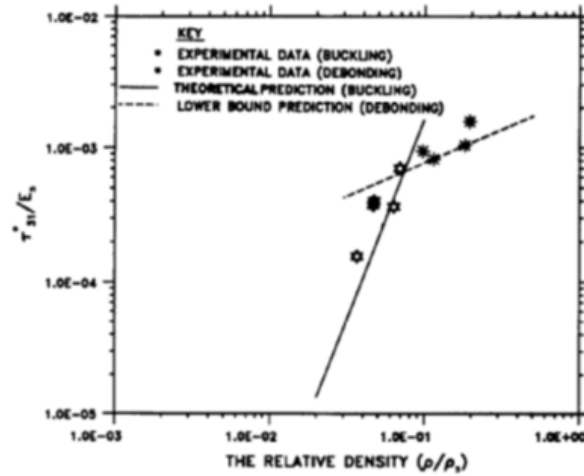


**Figure 1-6 Failure stress normalized by E [10].**

They have also concluded that collapse of honeycombs was through buckling and debonding. Based on these findings, Lee [11] identified the regions corresponding to various deformation modes in the stress-strain curves of hexagonal honeycombs and put forth a generalized collapse trend for hexagonal honeycombs as illustrated by Figure 1-7 Phases of honeycomb collapse under compressive loads [11].

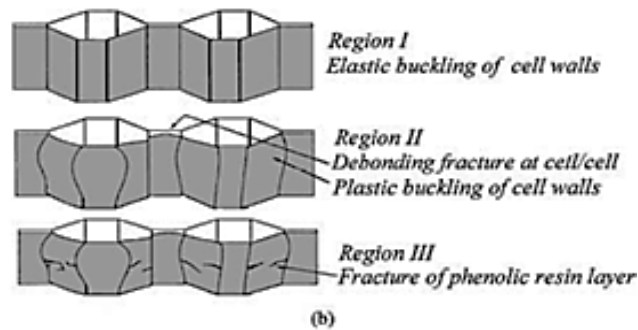
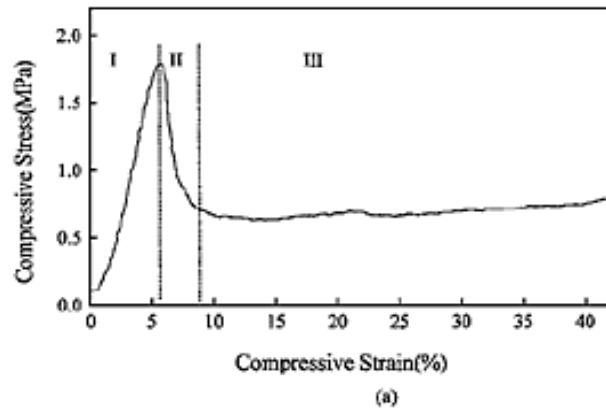


Figure 1-7 Phases of honeycomb collapse under compressive loads [11].

### Effect of Defects on Honeycomb performance

The effect of non-periodicity on honeycomb performance has been studied by Lorna and Gibson, [12]. They concluded that the strength of Voronoi honeycombs is approximately 30% less than periodic honeycombs. Based on observations, it was inferred that any kind of non-periodicity in microstructure would tend to decrease the strength of the honeycombs. Further in the same work it was suggested that the upper limit of strength for cellular materials in general could be defined by periodic microstructure.

Gibson and Ashby [3] have mentioned that their unit cell models overestimate the yield stress of metallic honeycombs (by as much as 50%). It was reasoned that this

difference was due to the variations in cell geometry of commercially available honeycombs that were unaccounted in their models. Papka and Kyriakides [13] found that the strength of honeycombs as predicted by Finite element models is around 15% greater than that of experimental values.

This was attributed to randomly distributed defects in commercial honeycombs. The importance of regular cell geometry is emphasized [14] by the fact that localized deformation is initiated at the regions of broken cell walls or missing cell walls due to near field strain magnification [15].

### **Response of Honeycombs to Multi-axial and inclined loading**

Experimental studies have been carried out on the effect of multi-axial loading and combined proportional and non-proportional loading on the out of plane properties of Honeycombs [16-19]. Doyoyo and Mohr [20] studied the collapse behavior of the honeycomb microstructure under combined loads. Petras and Sutcliffe [19] used a modified Arcan's setup in their study of the failure of honeycomb samples under oblique loading. In their experiments, they subjected Nomex honeycomb samples to oblique loads by changing the orientation of the honeycomb axes with respect to the normal loading direction; shown in Figure 1-8. A linear failure criterion for honeycombs under the influence of shear and compressive stresses was proposed. Their results show a significant decrease in the peak strength of the honeycombs with increase in loading angle  $\varphi$  (Figure 1-9). However, their study was confined to the elastic collapse regime of honeycombs.

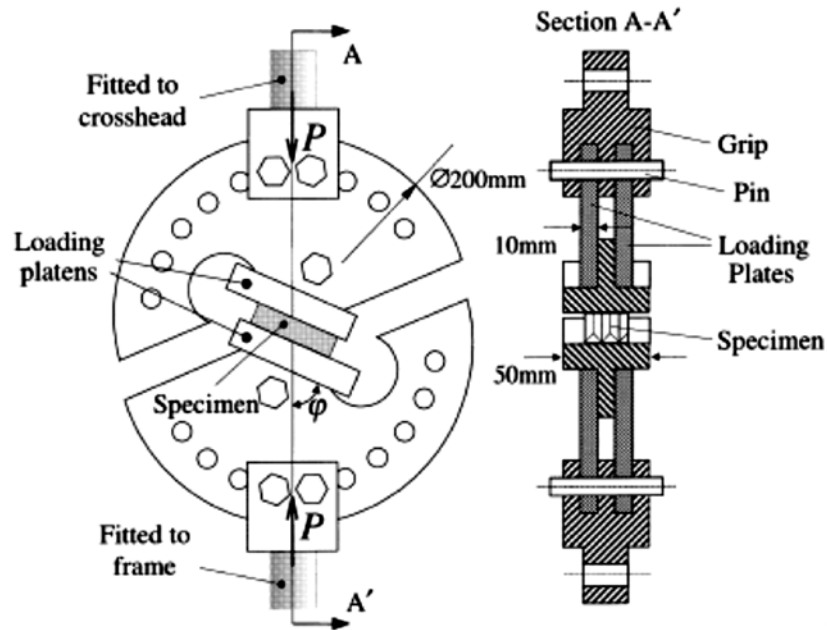


Figure 1-8 Modified Arcan's apparatus used to apply inclined loads [19].

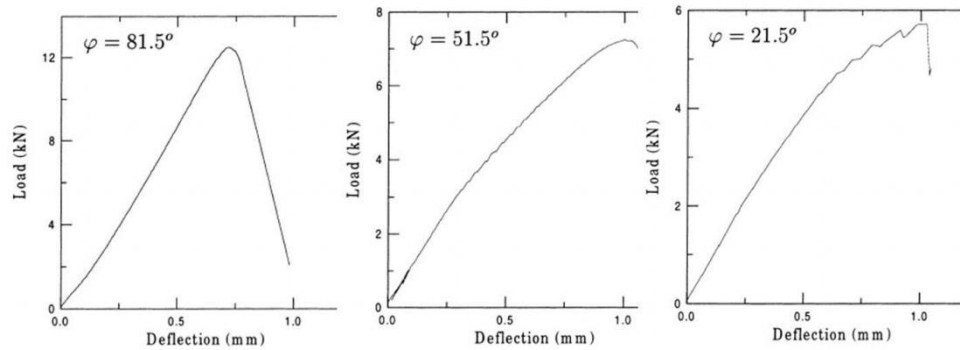
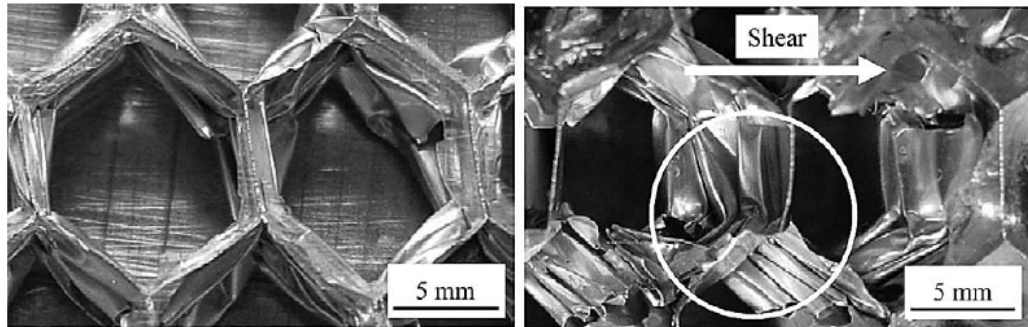


Figure 1-9 Results showing the decrease in peak strength of aluminum honeycombs with increasing load inclinations.[19].

Papka and Kyriakides [16] studied the in-plane biaxial crushing of honeycombs and also simulated the same. Kobayashi *et al.* [21] studied the effect of strain rate on Polypropylene (PP) and Polyethylene terephthalate (PET). They concluded that the strain rate response of the cores is strongly dependent on the strain rate behavior of the core materials. Secondly, it was also mentioned that increasing the core thickness alone proportionally increases the mechanical energy absorption. This implies that a double

layered or triple layered core would absorb as much as three times more energy in comparison to a single layer for a similar increase in weight.

Hong et al [17] investigated the response of aluminum honeycombs subjected to compression dominant combined loads. Honeycombs in various configurations or angular orientations of the material axes to the direction of shear load were tested. A non-normal plastic flow behavior and a reduction in normal crush strength of the honeycombs were noticed in comparison to pure compressive loading conditions. The shear stress ratio and the in-plane orientation angle  $\beta$  were emphasized as key parameters influencing the energy absorption rate. An inclined stacking pattern [17] was seen in specimens crushed under combined loads. Honeycombs compressed uni-axially, buckle and fold with each fold one on top of another. When subjected to inclined loads the stacking is skewed as shown in Figure 1-10



**Figure 1-10 Normal Stacking pattern (Left) and inclined stacking pattern (Right) in honeycombs.**

All of the above works mentioned excepting [19] focus on response of honeycombs to explicit combined loading conditions. There is very little data in literature with respect to the effect of inclined loads on honeycombs and this is in the subject of the present work. An elegant approach was taken to understand the effect of

oblique loading on honeycombs by the way of subjecting skewed honeycombs sections to normal loads. These experiments resemble the methods of Petras *et al.* [19].

## **Metallic Glasses**

Metallic Glasses are amorphous metals which exhibit the unique properties of glass [22]. Their lack of crystallinity has been credited to the non-existence of grain and phase boundaries. They exhibit very high yield strength with some of the cobalt based bulk metallic glasses exceeding 5GPa [23], and this can be correlated with their Young's modulus [24]. Figure 1-11 from Ashby *et al.* [24] shows that metallic glasses have very high resilience (region bound under grey lines); emphasizing their very high capacity to store mechanical energy in comparison to other metals.

Recognizing their high resilience and ultra-high yield strength, the potential of metallic glasses in creating new structural materials was brought to light in prior works, of which, Greer (2009) [25] is noteworthy here. Chen *et al.* [26] attributed the ultra-high plasticity of certain Zr based bulk metallic glasses to nano-crystallization which effectively curtails strain softening. This phenomenon induces plastic flow within shear bands resulting in extraordinary plasticity and strain hardening. Further, it was suggested that this finding could be an effective way to improve the ductility of monolithic metallic glasses.

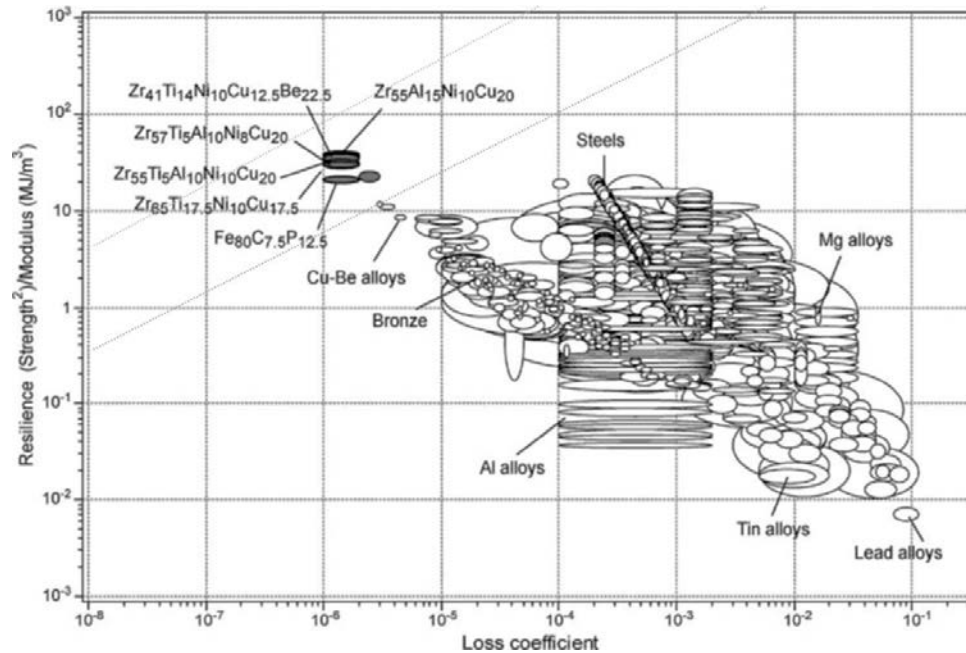


**Figure 1-11 Resilience  $\sigma_2y / E$  plotted against loss co-efficient  $\eta$  for 1507 metals, alloys, metal matrix composites and metallic glasses [24].**

Brothers and Dunand 2007 [27] found that with the increase in porosity of metallic glasses, the formation of shear bands is steadied or reduced, thereby yielding noticeable compressive strains as high as 80%. Although with this there is a decrease in strength and stiffness, there is an increase in ductility resulting in higher mechanical energy absorption and obvious weight reduction. Inoue *et al.* [23] reported higher specific strengths in metallic glass in comparison to Bulk Metallic Glasses.

### **Metallic Glass Honeycombs**

Amorphous metal foams have size restrictions arising from limitations of the current manufacturing methods and the base material. A radical solution to this problem was proposed by using a metallic glass, and an adhesive based manufacturing technique to create a first of its kind low density amorphous honeycomb [1, 28]. The material used was commercially available Metglas 2826 MB. The honeycomb structure eliminates the

size restrictions faced in foaming; giving a product that is suitable for a variety of mechanical energy absorption applications. The advantages of this honeycomb material in a dynamic impact environments has already been verified [29]. These amorphous honeycombs formed have cells in the shape of teardrops making use of the inherent elastic property of the base material.

The mechanical properties of teardrop honeycombs have been studied under quasi-static loading conditions along all three material directions [1, 28]. They were tested as mechanical energy absorbers in fiber fabric composite body armor panels and subjected to ballistic tests against Level-III threats (bullets travelling at 840m/s). The tests were successful to a great extent in reducing the Back Face Signature (BFS) of the armor panels. A significant reduction in BFS of 23% was observed in comparison to the base line panels [2]. It was speculated that streamlining the manufacturing method to bring about a defect free structure would vastly improve the honeycomb properties and in turn, further reduce the BFS.



**Figure 1-12 Armor panel with Tear Drop lattice core which successfully stopped four bullets [2].**

To form the TD Lattice a bottom-up method of manufacturing was followed wherein cells were formed one at a time by bending the ribbon in the shape of a tear drop and then using an epoxy to hold the shape [2]. A rail and track technique (Figure 1-13 and Figure 1-14) was used to make Tear-Drop lattice rows.

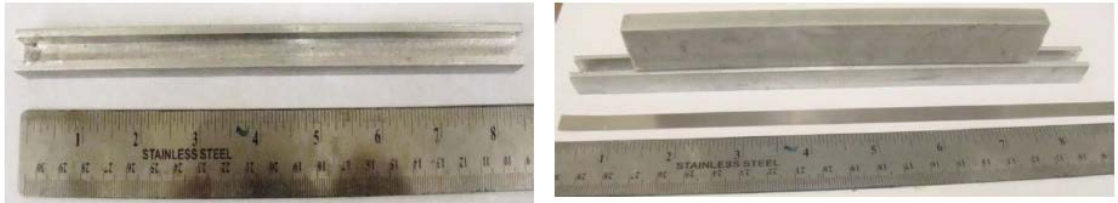


**Figure 1-13 Track and slider used for making TD lattice rows.**

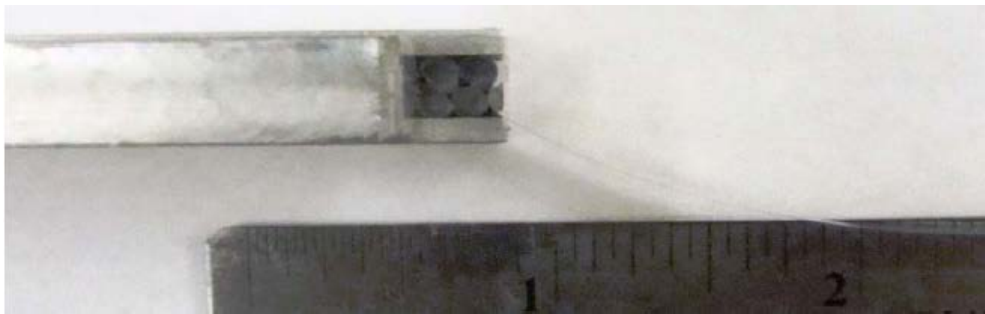


**Figure 1-14 Tear Drop lattice ribbon formed by using the width of the ribbons as the height [2].**

The geometry itself is such that each cell has to be made with the support of the adjacent cell to obtain a continuous row. Required numbers of rows were then bonded together in a staggered manner using a two-part epoxy, in this case Scotch-Weld DP-110 adhesive to obtain a plate of required area.

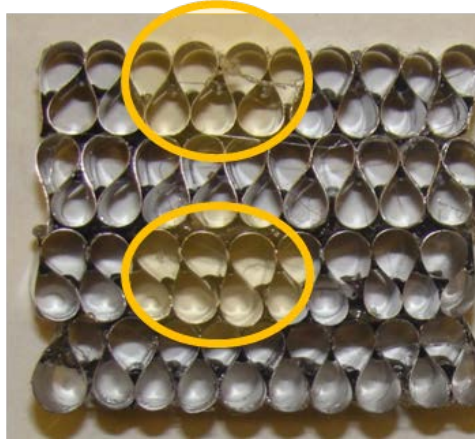


**Figure 1-15 Non-uniformity in cell shape and size seen in a small Folded Tear-Drop Lattice sample [2].**

The problems inherent to this method of manufacturing are: (i) maintaining straight cell walls (cell axis inclination towards  $X_2$  (Figure 1-16)) (ii) height consistency from cell to cell (Figure 1-16) (iii) stability of cell shape and size (Figure 1-15) and (iv) warping. The quantification and elimination of resulting defects is pursued as a part of the present work



**Figure 1-16 Pronounced Cell height misalignment in Folded Metallic Glass Honeycombs[2]**

## CHAPTER II

### 2. MATERIALS and METHODS

#### 2.1. Metallic Glass Ribbon-MetGlas 2826 MB

MetGlas 2826 MB, Fe<sub>45</sub>Ni<sub>45</sub>Mo<sub>7</sub>B<sub>3</sub>, a ferromagnetic glass alloy is a product of Allied Signals now MetGlas Inc. (USA) [30]. It is manufactured as thin metallic ribbons.

The physical properties of the ribbon are as tabulated in Table 1.



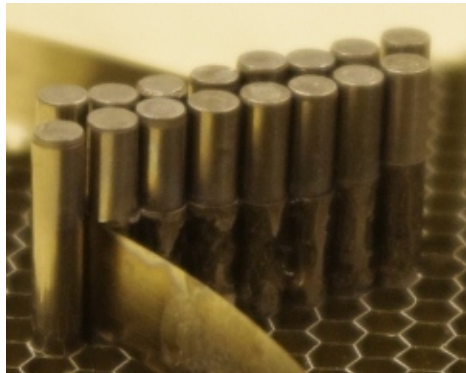
Figure 2-1 Fe<sub>45</sub>Ni<sub>45</sub>Mo<sub>7</sub>B<sub>3</sub> - MetGlas 2826 MB.

Table 2-1 Physical properties of MetGlas 2826 MB [31].

Physical Properties	Values
Thickness (mils)	1.15 (29 $\mu\text{m}$ )
Width (mm)	8
Density ( $\text{g}/\text{cm}^3$ )	7.90
Vicker's Hardness (50g Load)	740
Tensile Strength (GPa)	1-2
Elastic Modulus (GPa)	100-110
Crystallization Temperature ( $^{\circ}\text{C}$ )	410

## 2.2. Continuous Ribbon Winding Method for manufacturing Tear Drop Lattice honeycombs

To begin with, a hexagonal AL 5052 panel of approximately 23,000 mm<sup>2</sup> (6 in<sup>2</sup>) area is used as a base plate. Dowel pins of 3.175 mm (0.125 in) diameter are inserted into the cells. A known length of Metglas 2826 MB ribbon is taken and wound around the dowel pins as shown in. Figure 2-2. The same step for a longer teardrop lattice row is shown in Figure 2-3.

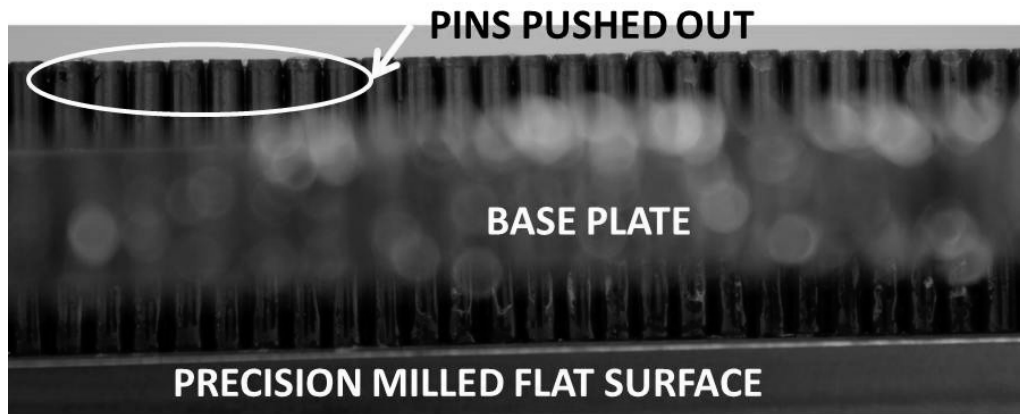


**Figure 2-2 Ribbon wound around dowel pins.**

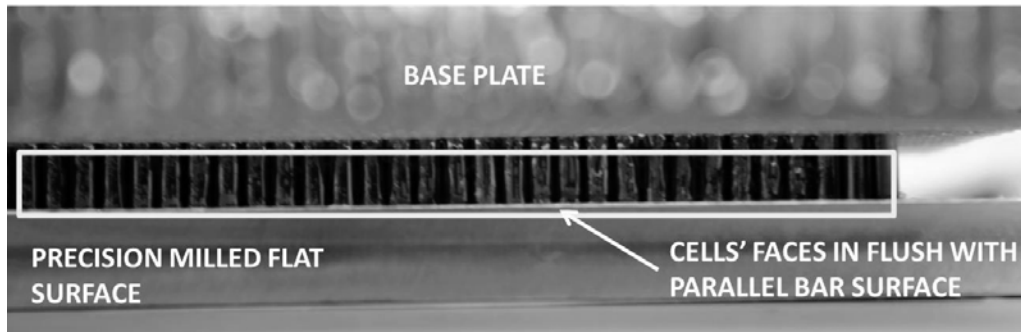
Then, a desired adhesive is applied at the cell boundaries. In the case of a hot-melt adhesive; hot air is blown over the sample to melt the applied adhesive; allowing it to penetrate the gap between the cells and bond better. The heat retained by the steel pins keeps the glue in a molten state for about 3 minutes. During this time the base plate is inverted and the dowel pins are pushed out gently until the ribbon walls are in contact with the table surface (Refer Figure 2-4 (a) and (b)). This step negates the chances of cell height misalignment.



Figure 2-3 A long tear-drop lattice row on application of adhesive.



(a)



(b)

Figure 2-4 (a) and (b) Base plate inverted; cells' faces flush with flat surface.

Again, hot air is blown to re-melt and settle the adhesive and excess of it is removed using a hot tip. On curing, the dowel pins are pulled out and the tear-drop lattice row is lifted off the base plate. The excess length of the ribbon is trimmed. Often

excess adhesive bonds the pins to the cell walls which make it difficult to pull them out and results in cell wall deformation in the base plate. So the base plate has to be carefully checked after each MGH row is made. However, with two or three uses a row of the base plate becomes unusable. The base plate also bends while pulling giving rise to a slight height misalignment.

Approximately 14 cm of ribbon is required to make a 25 mm (1 in) row. The foil thickness of the base plate was chosen such that it is thin enough to minimize the gap to be filled by the adhesive at the same time thick enough to resist deformation while pulling out the dowel pins. The foil thickness is 0.04 mm in this case.

Scotch weld DP 110, a two part epoxy is applied along the rows' side walls and then the required numbers of rows are stacked with cells in contact in a staggered manner to form a plate of required dimension. These plates are aligned between two precision milled parallel bars and a 0.75 Kg weight plates were used to apply pressure along the vertical and horizontal directions and allowed to cure. Figure 2-5 and Figure 2-6 show teardrop lattice plates of different sizes implying scalability of the process.

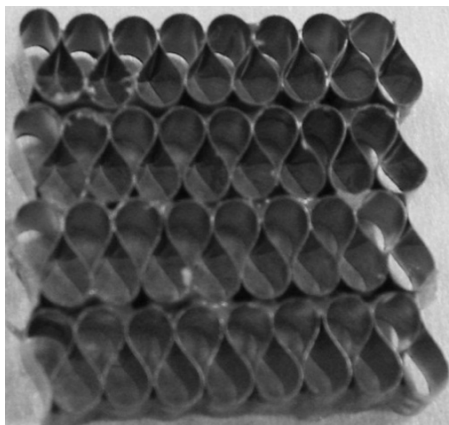


**Figure 2-5 A 820 mm<sup>2</sup> TD lattice sample.**



**Figure 2-6 A 5 in x 3 in Metallic Glass honeycomb plate.**

It is noted that the adhesives used previously (commercially available hot-melt and DP 110 a two part adhesive) have been retained in this method of manufacturing. Manufactured honeycombs were also tested using cyanoacrylate adhesive, in this case commercially available super glue, for cell bonding.

Row height misalignment is a defect that is unavoidable in manual methods of manufacturing and depends on factors like evenness of the surface on which the rows are stacked and flatness of the base plate. Although barely noticeable in carefully made samples, height misalignment has to be removed to ensure that the specimen faces are flush with the platens' surfaces for carrying out relevant compression tests. Therefore the excess glue can be removed using 400 grit sand paper and the sample faces polished using a fine 600 grit sand paper to obtain more parallel faces. Polishing also aids in keeping the sample height misalignment to a minimum

### 2.3. Properties of Adhesives used in manufacturing TD lattice honeycombs

Motivated to find a better adhesive for TD lattice honeycombs, a commercially available cyanoacrylate gel (Scotch super glue gel) was chosen for cell wall bonding. The choice was based primarily on gap filling properties, the ease of application, and cost. Moreover the strength of the adhesive had to be comparable or more than that of the hot-melt. Therefore the strength of the super glue was measured by conducting adhesive shear strength test and compared to that of the hot-melt.

#### Adhesive shear strength test

The overlap shear strength of the Cyanoacrylate adhesive was tested according to ASTM D1002 “Standard Test Method for Apparent shear strength of single-lap-joint adhesively bonded Metal Specimens by tension loading (Metal-to-Metal)”.

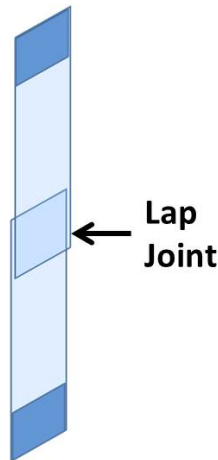


**Figure 2-7 A schematic representation of Lap jointed ribbon specimens.**

Lap jointed test specimens were prepared as shown schematically in Figure 2-7 and were cured for about 24 hrs. Self-aligning grips were used to ensure uniform loading only along the specimen length. Figure 2-8 shows a Super glue Lap jointed sample under

tensile loading. Five samples were tested and stress-strain plots were obtained from cross head displacement and load data. Average shear strength values were noted



**Figure 2-8 Super glue lap joint shear strength test.**

## **2.4. Quasi-Static Compression Testing of Honeycombs**

Considering the anisotropic nature of honeycombs, MG Honeycomb being a new product was studied along all three material directions. However, Aluminum honeycombs were studied along the  $X_3$  direction only.

### **Out of plane compression testing of Metallic Glass Honeycombs**

ASTM C365/C365M-05 (“Standard test method for Flatwise Compressive properties of Sandwich Cores”) was followed for all quasi-static compression tests. Figure 2-9 shows a Tear drop lattice sample under quasi-static compression.

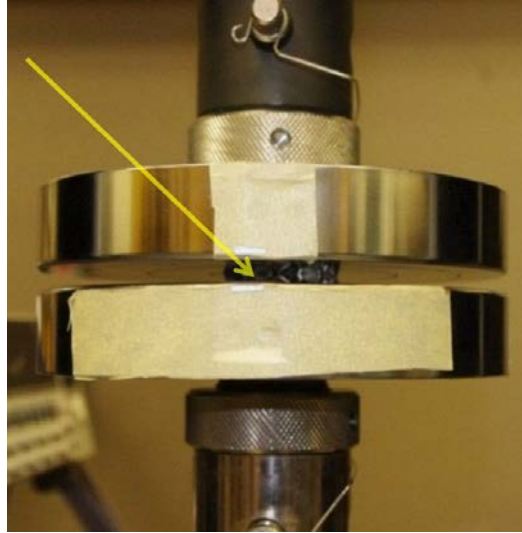


**Figure 2-9 Tear Drop Lattice Honeycomb under quasi-static compression between two platens.**

The sample size and the cross-head displacement (0.5 mm/min) of the universal testing system (UTS Instron 5582), conform to the above mentioned standard. The size of the tested samples was 820 mm<sup>2</sup>. Five samples of each type-Hot-melt and Cyanoacrylate (super glue) were tested and, stresses and strains were obtained from load and displacement data.

### **In-plane compression testing of MG Honeycombs**

The same procedure used for the X<sub>3</sub> direction tests was followed for the X<sub>1</sub> and X<sub>2</sub> directions. The sample dimensions were 26 mm x 27 mm x 8 mm for both the in-plane cases. A stress vs. strain graph was plotted from load and extension data and corrected for compliance. Since the sample width was small (8mm) a thin double sided tape was stuck to the bottom compression platen for better sample alignment.

## Compression testing of Aluminum honeycombs

Aluminum honeycombs, of 0.13 g/cc density or a relative density of 4% were used for these tests. The samples were approximately 830 mm<sup>2</sup> in cross-sectional area. It was ensured that the specimens did not have broken or damaged cells to prevent localized stresses. They were trimmed to remove burrs and excess cell wall extensions. Table 2-2 gives the specifications of Metallic glass and aluminum samples tested.

**Table 2-2 Specifications of Honeycombs tested**

Honeycomb Material	Density g/cc	Foil Thickness (t) mm	Height (h) mm	Cell Size (l) mm	Cell Shape	Relative density
AL 5052	0.13	0.002	10	3.175	Hexagon	4%
Fe <sub>45</sub> Ni <sub>45</sub> Mo <sub>7</sub> B <sub>3</sub> (Metallic Glass)	0.29	0.001	8	3.175	Teardrop	3%

## 2.5. Comparison of Geometry of Old and New teardrop lattice Honeycombs using Micro Computed Tomography

The geometries of Old and New tear Drop lattice samples were compared to understand the impact of defects on the strength of teardrop honeycombs. They were analyzed using Micro Computed Tomography A 25.4 mm length tear drop lattice row was fixed to the stage of a Skyscan 1172 Micro-CT machine, with its cell axis in line with the axis of the stage. The specimen face was aligned precisely in flush with the stage surface. The sample was exposed to 56KV X-rays with Al 0.5mm filter. Raw image slices were obtained using a high resolution camera (2048 x 2048). The pixel size

of the image slices or the radiographs was 35  $\mu\text{m}$  and they were reconstructed using the Skyscan software to remove artifacts.

A 3-D rendering was obtained by stacking the reconstructed radiographs using Amira. The same procedure was repeated on a folded sample. Geometry analysis was carried out using Image J software. The cell axis misorientation was measured for seven cells in both the folded and wound samples, and the average misorientation from normal was tabulated

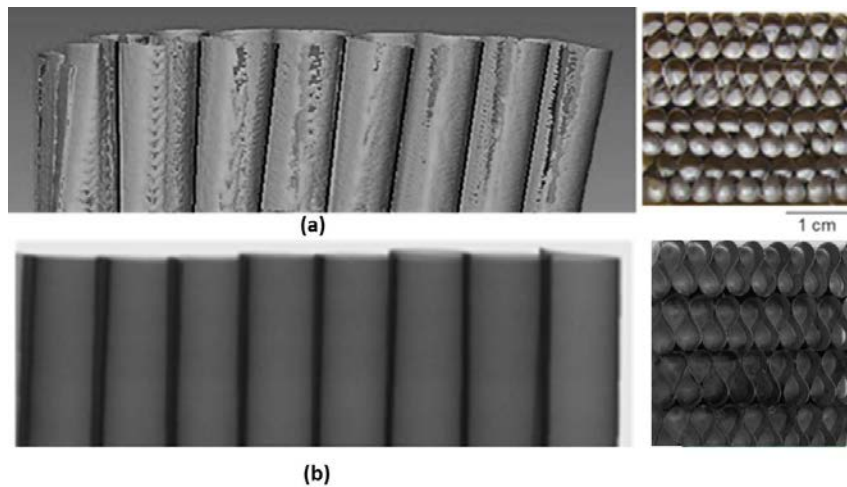


**Figure 2-10 A front view of reconstructed radiographs (a) folded sample (b) wound honeycomb samples.**

## **2.6. Quasi-Static compression testing of honeycombs with inclined cell axis.**

### **Procedure**

From the Micro-Ct scans it was surmised that cell axis misorientation was a reason behind the significant difference in yield and crush strengths of the folded and wound MG Honeycombs. This misorientation in the folded MG honeycomb was along the  $X_2$  axis, which was the weakest direction. It was also speculated that with increase in

cell axis inclination, the strength of the honeycomb would be a combination of the *strength along the normal* and the *strength along the direction of inclination*.

Due to the limitations in machining of MG honeycombs, aluminum honeycombs were used to test the hypothesis. Skewed aluminum honeycomb (specifications in Table. 2) sections with cell axes inclined towards  $X_1$  direction- $X_1$  being the weakest for aluminum honeycombs- were subjected to normal compressive loads. (Figure 2-11)

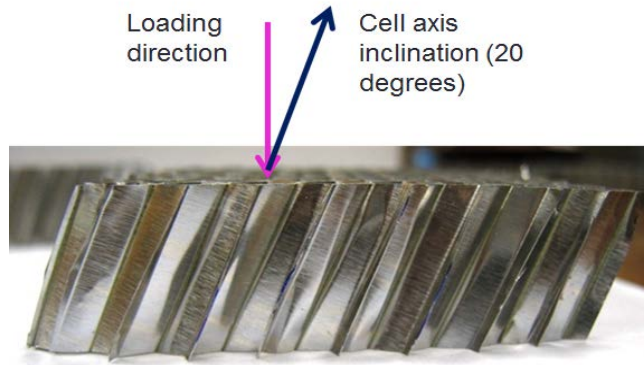


**Figure 2-11 Skewed aluminum honeycomb section.**

**Table 2-3 Specifications of honeycomb used for making skewed sections.**

Honeycomb Material	Density g/cc	Foil Thickness (t) mm	Height (h) mm	Cell Size (l) mm	Cell Shape
AL 5052	0. 07	0. 0015	15	4. 7	Hexagon

This experiment was repeated at increasing cell axis inclinations. Samples with cell axis inclinations (T-L plane inclination) of 90, 87, 85, 83, 80, 75, 72.5, 71.5, 70, 65, 60 and 0 degrees were tested at quasi-static strain rates. Stresses and strains were calculated from load and extension data as in previous cases. It is to be noted that a cell axis orientation of 90 degrees corresponds to the  $X_3$  direction and 0 degrees corresponds

to the  $X_1$  direction. One sample for each angle was tested and the repeatability is shown through a scatter graph of Crush strength vs. Cell axis inclination.

### Sample preparation

Aluminum Honeycombs were cut into 2 sq in cross sections on a band saw. The side walls were sanded to remove burrs. The honeycomb sections were then wrapped in sheet metal and covered with water proof tape or duct tape along the lateral and longitudinal directions to prevent the cell walls from buckling while machining. Waterproof tape binds the sheet metal cover to the honeycomb sections and ensures a strong hold even when in contact with continuous coolant spray.

As the next step one of the cut-off saw's vise jaws was removed and the other one was set to the required angle. The honeycomb section to be machined was then clamped firmly to the jaw using a C-clamp, as shown in Figure 2-12. A flat wooden plate was placed between the honeycomb and the C-clamp jaw to prevent damage to cells. Precision angle blocks were used to set the cutting angles (Figure 2-13).

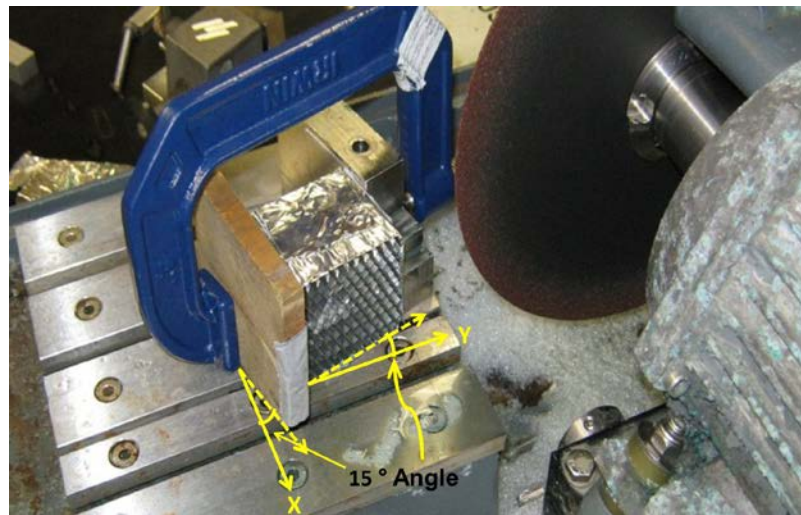
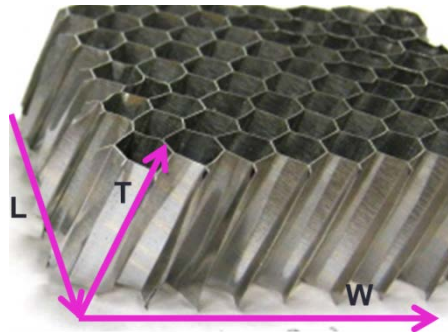


Figure 2-12 Honeycomb section mounted at fifteen degrees on a cut-off-saw.



**Figure 2-13 Precision angle block used to set the vise jaw angle.**

Cuts were made at a distance of 16 mm to obtain skewed sections of 16mm thickness. The sections prepared were then sanded to 15mm to obtain perfectly parallel faces. Test pieces of 1764 sq mm were cut out carefully from the sanded pieces and studied under normal compressive loads. There were no broken or crushed cells in the test samples. It is to be noted that the cells axes are inclined towards the  $X_1$  direction or perspective the **L-T** plane is inclined as shown in Figure 2-14.



**Figure 2-14 Honeycomb with inclined cell axes.**

## CHAPTER III

### 3. RESULTS

#### 3.1. Features of continuous ribbon winding method

The new continuous ribbon winding technique developed for manufacturing tear-drop lattice honeycomb samples has significantly reduced structural defects compared to those seen in folded MG honeycombs. The following are the noteworthy advantages of the continuous ribbon winding technique when compared to the older folding method of manufacturing MG ribbons.

- 1) Cell axis misorientation is eliminated.
- 2) Uniform cell size and shape is achieved.
- 3) It provides ease to experiment with adhesives.
- 4) Cell height misalignment and warping are minimized.

The disadvantages are;

1. Base plates and pins of different sizes are required to make honeycombs of bigger cell sizes.
2. It is still a manual method of manufacturing and is not suited for large scale production.

### 3.2. Properties of Adhesives used in Tear Drop lattice honeycombs

Two types of adhesives were chosen to make metallic glass honeycomb samples the previously used hot-melt from Adtech Inc. and a Scotch superglue gel from 3M. The shear strength of super glue was compared to that of the hot melt by analyzing stress-strain data from Adhesive shear strength tests; described in Section 2.3. From the stress-strain curves for the hot-melt and the super glue (Figure 3-1), it is seen that the shear strength of the super glue is slightly higher than that of the hot-melt.

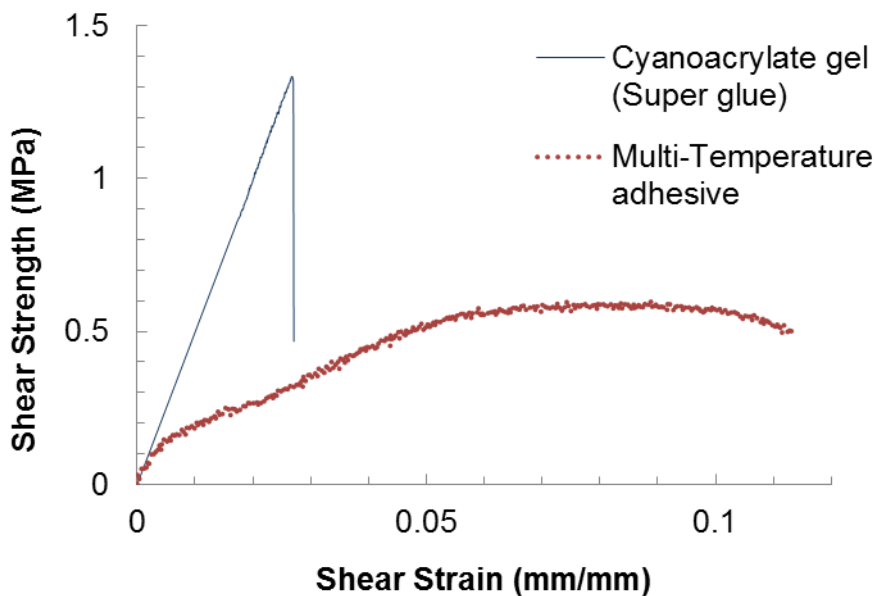


**Figure 3-1 Comparison of apparent shear strength of Cyanoacrylate gel and Multi temperature hot melt**

The shear strength of the super glue was 1.7 MPa and that of the hot-melt was 0.6 MPa. The elasticity of the super glue is lesser as indicated by the smaller extension it has undergone before failure.

### 3.3. Mechanical properties of Metallic glass honeycombs

#### Out of plane properties of Metallic Glass Honeycombs

The comparison of stress-strain curves for the wound MG honeycombs and Aluminum honeycombs-presented in Figure 3-2-shows a significant improvement in MG honeycomb's performance as compared to the folded MG honeycombs.

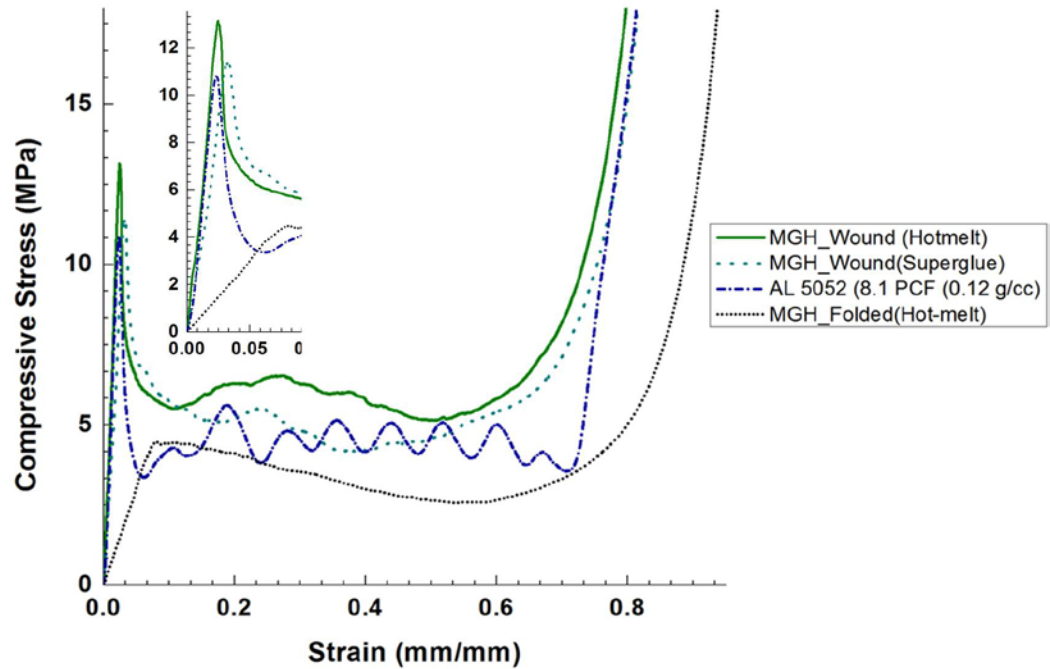


**Figure 3-2 Stress-Strain plot comparing MG honeycombs to aluminum honeycomb**

The honeycombs manufactured using Superglue show a 10% lesser peak and 20% lesser crush strengths as compared to the hot-melt samples. The densification achieved in case of MG honeycombs was in the range of 65-72% strain and for aluminum honeycombs it was in the range of 70-72%. Comparison of crushed MG samples and aluminum samples show: extensive de-bonding both at the nodes and across the rows, and also an irregular collapse pattern in the former case. Whereas in the case of the latter

there is no bond failure and the collapse pattern is stacked and symmetrical as shown in Figure 3-5



**Figure 3-3 Random collapse pattern and extensive bond failure in MG honeycombs**

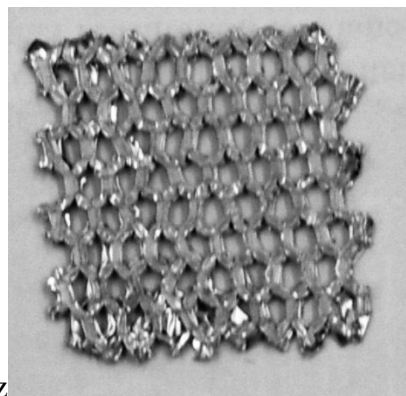


**Figure 3-4 Regular stacking pattern seen in crushed aluminum honeycombs**

This interesting behavior is further made evident by the relatively extended de-bonding region and a non-linear plateau for MG honeycombs as compared to aluminum.. The de-bonding region begins from the peak of the stress-strain curve to the beginning of the plateau [11] and for MG honeycombs it extends from 0.02 strain to almost 0.12 strain. The de-bonding region signifies the stage during collapse of honeycombs wherein the cell-cell bonds are broken[11]. For aluminum honeycombs, de-bonding occurs over a

relatively shorter extension-between 0.008-0.06 strains. An irregular plateau is seen for all the MG honeycomb samples as shown in Figure 3-5.

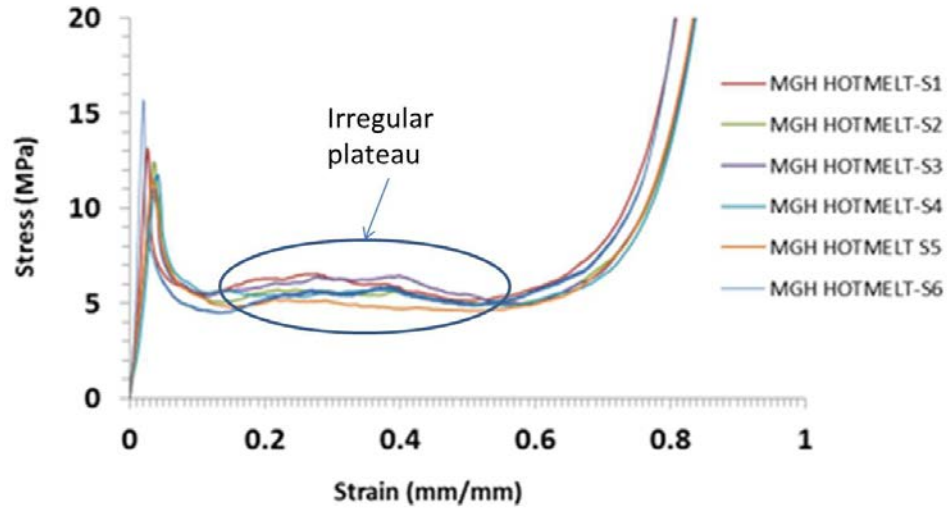


**Figure 3-5 Stress-strain curves for Metallic Glass Honeycombs indicating the irregular plateau**

From the stress-strain curves, the peak stress, plateau stress, elastic modulus, and mechanical energy absorbed for each honeycomb was obtained and is tabulated in Table 3-1. The energy absorbed is given by the area under the curves.

**Table 3-1 Peak Stress, Plateau stress, Young’s modulus and Energy absorbed for each honeycomb**

Honeycomb Type	Peak strength (MPa)	Crush strength (MPa)	Young’s modulus (GPa)	Energy absorbed (J/mm <sup>3</sup> )
Wound Metallic Glass (Hot-melt)	13.15	5.54	1	3.6
Wound Metallic Glass (Super glue)	11.35	4.88	0.4	3.29
Aluminum 5052 8. 1 PCF	10.8	4.40	2.3	3.23
Metallic Glass-folded	-	3.32	0.06	2.3

### In plane properties of Metallic Glass Honeycombs

Stress and strain curves (Fig.32) for the in-plane directions were plotted from load and extension data (Section. 2.4)

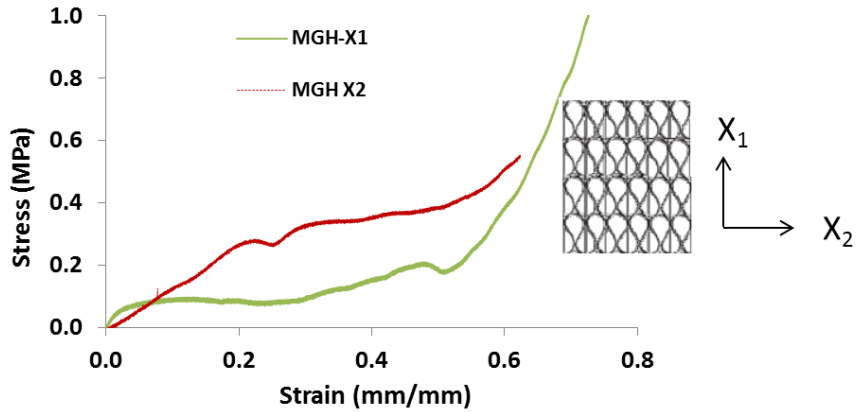


Figure 3-6 Stress-Strain data for wound MG Honeycombs along in-plane directions

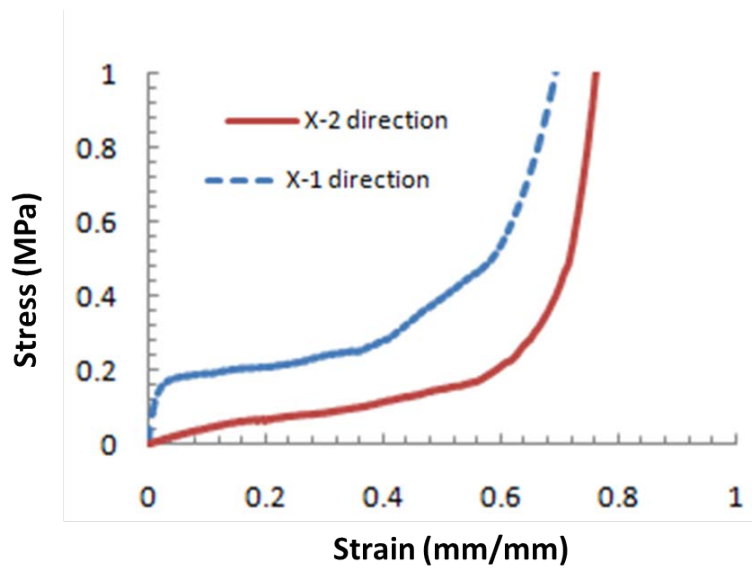


Figure 3-7 Stress-strain curves for folded MG honeycombs along the in-plane directions [2].

It is seen that wound MG Honeycombs are stronger along the  $X_2$  direction than along  $X_1$ . The plateau stresses for the  $X_1$  and  $X_2$  directions are 0.12 MPa and 0.34 MPa. The elastic modulus for the in-plane directions are 0.0024 GPa for  $X_1$  and 0.0013 GPa along  $X_2$ . The wound honeycombs are stronger than folded honeycombs along both the in-plane directions. The  $X_1$  strength of the folded MG honeycombs were higher than  $X_2$  direction strength. More samples need to be tested to arrive at a satisfactory conclusion on in-plane behavior.

### 3.4. Geometry comparison of folded and wound Metallic Glass honeycombs

The geometries of the folded and wound Metallic Glass Honeycomb samples were compared using 3-D volumetric renderings obtained From the Micro Computed Tomography scans- described in section 3.6. The measured cell wall inclinations over 7 cells are compared in Table 3-2

**Table 3-2 Cell axis misorientation in folded and wound honeycombs**

	Cell wall inclination in Degrees	
	Folded MG honeycombs	Wound MG Honeycombs
<b>Cell 1</b>	8.61	2.8
<b>Cell 2</b>	10.12	2.93
<b>Cell 3</b>	8.33	1.34
<b>Cell 4</b>	6.27	0.93
<b>Cell 5</b>	6.47	1.86
<b>Cell 6</b>	1.58	1.12

<b>Cell 7</b>	0.136	0.56
---------------	-------	------

The average cell wall inclination for wound honeycombs was  $1.5^\circ$ , whereas for folded honeycombs it was  $5.9^\circ$ . Moreover, a high degree of non-uniformity in cell morphology is observed in the folded honeycombs. In the wound honeycomb, the cell size and shape are significantly more uniform.

### **3.5. Effect of cell axis inclination on Honeycomb performance**

The effect of normal loads on honeycombs with inclined cell axis was studied by compacting skewed Aluminum honeycombs with different degrees of cell axis inclinations. The stress-strain graphs for skewed honeycombs sections are presented in Figure's 3-8 to 3-10. Figure 3-11 shows the stress-strain curves for sections having different cell axial orientations and Figure 3-12 shows the variation of crush stress and elastic modulus with cell axis inclination.

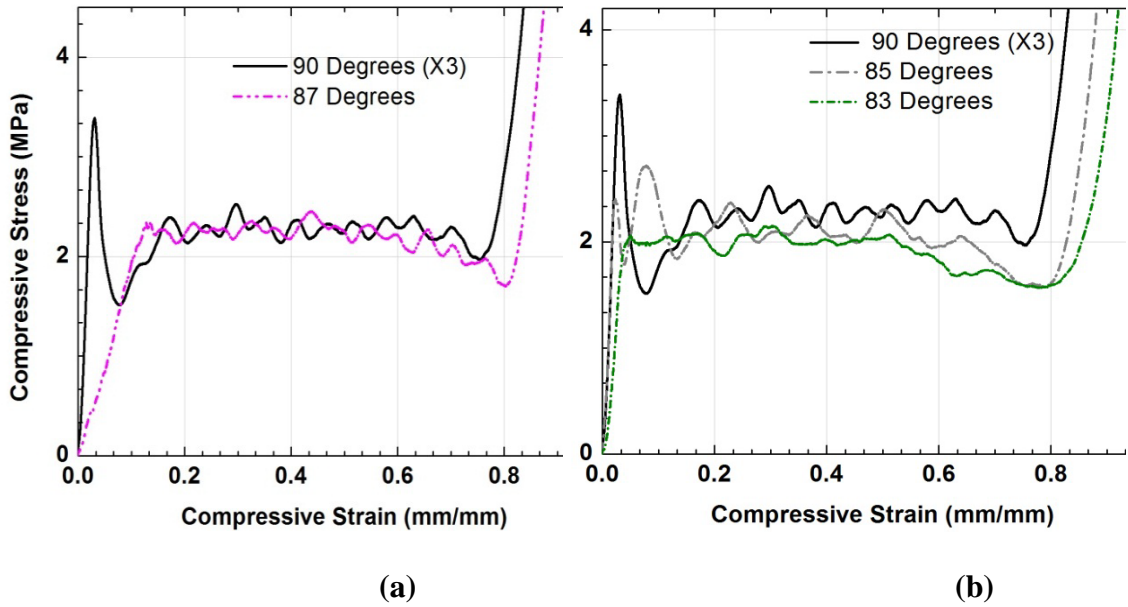


Figure 3-8 Plots for (a) 90°(X<sub>3</sub>) and 87° sections (b) 85° and 83° (Steep Drop in plateau stress)

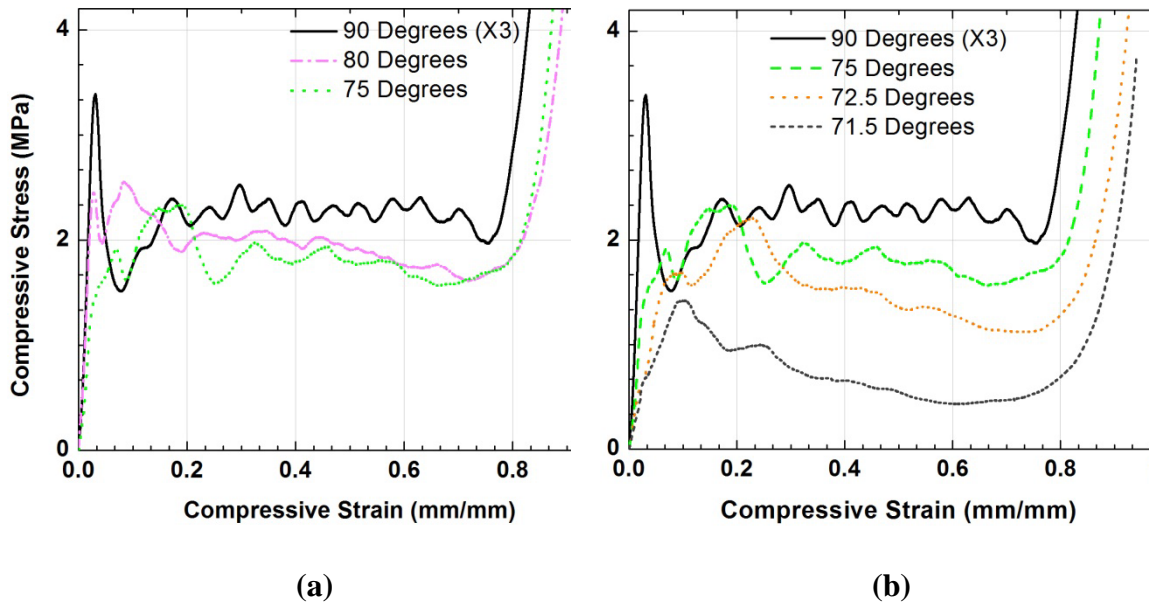
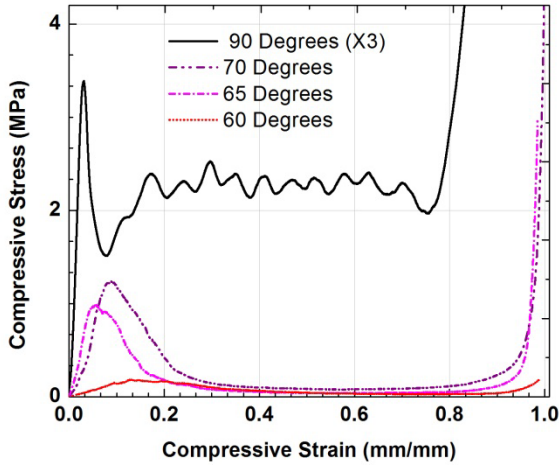
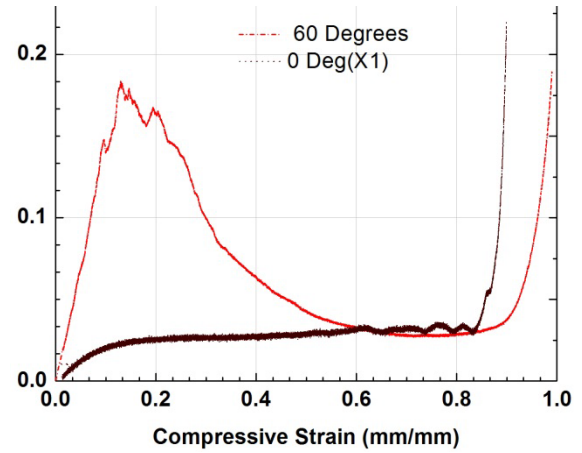


Figure 3-9 Plots for (a) 80° and 75° sections (b) 72.5° and 71.5° (Steep Drop in plateau stress)



(a)



(b)

Figure 3-10 Plots for (a) 70°, 65° and 60° sections (b) 60° and 0° (X<sub>1</sub>)

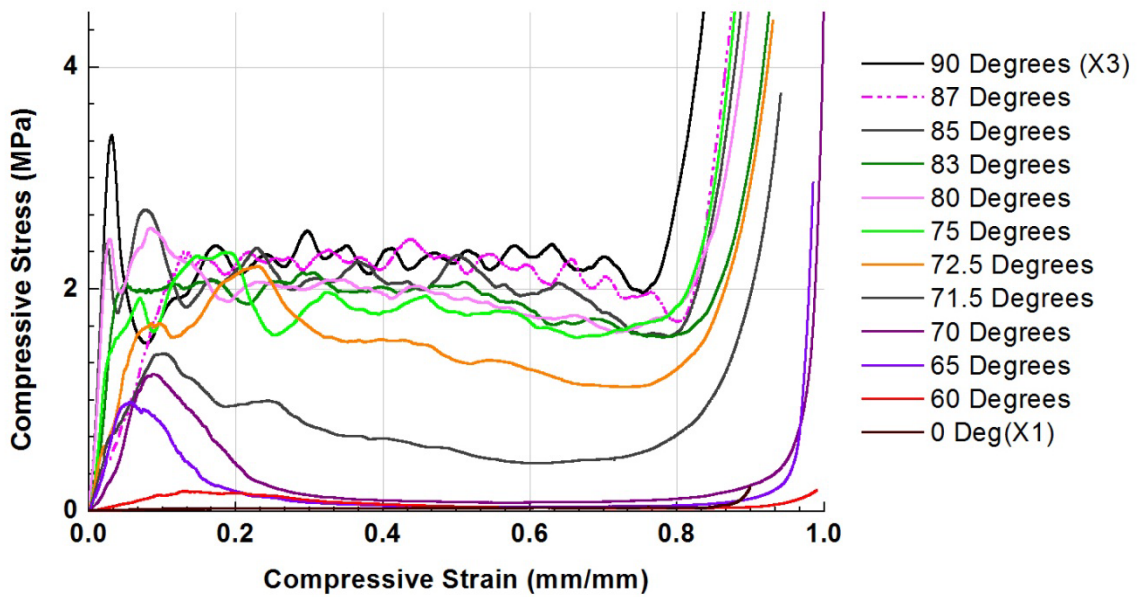
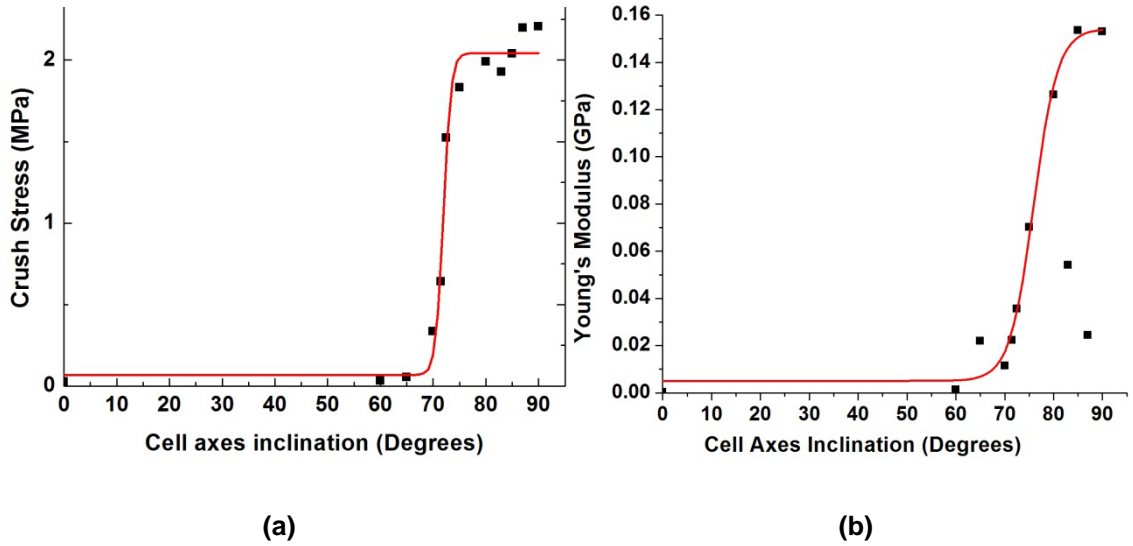


Figure 3-11 Stress-strain plot for all skewed sections



**Figure 3-12 Plot of (a) Crush stress Vs. Cell axes inclination (b) Young's modulus vs. Cell axes Inclination. (The error from the actual readings is  $10^{-3}$  MPa and  $10^{-3}$  GPa)**

The Young's modulus and plateau stress of aluminum honeycombs showed a decreasing sigmoidal trend with increasing cell axis inclination to normal. The transition is between  $72.5^\circ$  and  $71.5^\circ$ . A good sigmoidal fit for the variation of both modulus and plateau stress was obtained with  $X_3$  and  $X_1$  data points as the asymptotes. The curve for young's modulus variation is centered at  $76^\circ$  and the curve for the crush stress variation is centered at  $72^\circ$ . The regression ( $R^2$ ) for the variation of crush stress with cell axis inclination was 0.98. For variation of modulus with cell axis inclination; excluding the outliers at  $83^\circ$  and  $87^\circ$  the  $R^2$  value obtained was 0.99.

It is seen that from  $90^\circ$  onwards up to  $72.5^\circ$  inclination, the reduction in strength was around 30%. Below  $72.5^\circ$  a steep drop in plateau stress of 60% was seen. The difference in crush strength between honeycombs with straight cell walls and honeycombs with  $71.5^\circ$  cell axis inclination was 70%. From  $71.5^\circ$  onwards, the decrease in plateau stress is gradual and at  $60^\circ$  the honeycomb crush strength was 0.03 MPa, which is almost the same as the strength along  $X_1$  (0.028 MPa).

## CHAPTER IV

### 4. Discussion

#### 4.1. Properties of Wound Metallic Glass Honeycombs

Although MG honeycombs were compared with aluminum honeycombs of lower density, the relative density of the latter was higher. The relative density of MG honeycombs used here was 0.03 and that of the aluminum honeycomb was 0.04; a difference of 25%. This is in part due to the thickness of the MG ribbon being 29  $\mu\text{m}$ , which is significantly less than the foil thickness of the aluminum honeycomb's which was 50.8  $\mu\text{m}$ . The crush strength, peak strength and Young's modulus of the aluminum honeycombs tested along  $X_3$  direction concurs with the data sheet values [32], validating the comparison.

Wound MG honeycombs have a 40% higher plateau stress than folded MG honeycombs along the  $X_3$  direction. Moreover folded MG honeycombs were stronger along the  $X_1$  (perpendicular to the ribbon) direction than the  $X_2$  (parallel to the ribbon) direction, whereas it was vice versa in wound MG honeycombs.

These significant improvements in the performance of metallic glass honeycombs can be attributed to elimination of cell axis misorientation made possible by the continuous ribbon winding technique. Contributions from other factors like uniform cell

size and elimination of row height misalignment are the other factors that have not been quantified.

The role of cell inclination is shown by the results of skewed honeycomb compression tests. For a cell axis inclination of 15 degrees, the drop in honeycomb strength is 30%. This is also the maximum inclination seen over a 26 mm length of the folded teardrop lattice honeycombs. Now, the difference in strength of 40% between the wound and folded MG honeycombs can be attributed to the difference in cell axis inclination of 15° along with the other cellular defects accounting for the remaining 10%.

Metallic glass honeycombs made using cyanoacrylate adhesive show almost the same performance as that of the honeycombs made using hot-glue. But bond failure was seen in the former samples over a period of time. Considering that the shear strength of the cyanoacrylate is higher than that of the hot-melt, low T-peel strength of the super glue which is generally the case with most cyanoacrylate adhesives [7, 33] can be the reason behind this observed failure. The elastic modulus of the cyanoacrylate honeycombs is slightly higher. Higher modulus implies higher resilience which is a desirable property in honeycombs. Therefore stiffer epoxies would be better suited for honeycomb application. Weak adhesive bonds reduce the strength of MG honeycombs and this could also be the reason behind irregular plateau and variation in Young's modulus.

The off-axis sections tested had cell wall inclinations along the  $X_1$  direction which is the weakest direction for aluminum honeycombs. Although folded MG honeycombs were inclined towards the  $X_2$  direction, the aluminum honeycomb sections tested were inclined towards the  $X_1$  direction (refer Figure 2-10). The reason behind this is, as

previously mentioned; the folded MG honeycombs were weakest along  $X_2$ , which corresponded to the weakest direction of aluminum honeycombs  $-X_1$ .

## 4.2. Inclined Honeycomb Section tests

The peak strength (bare compressive strength) of the tested honeycombs sections with normal cell walls is 3.4 MPa which concurs with data sheet value of 500 ksi [17], thus validating the experimental method followed. The decrease in strength with cell axis inclination concurs with the results of Petras *et al.* [19]. In 19 it is shown that there is 40% drop in peak strength of Aluminum honeycombs between loading at  $81^\circ$  inclination and loading at  $51^\circ$  inclination. But the density of the honeycomb tested was higher when compared to the present case by 45%. From this, it is inferred that the percentage decrease in strength with increasing angles of loading depends on honeycomb density.

Normal loading on honeycombs with oblique cell axis generates the same conditions as oblique loading on honeycombs with normal cell axis. Now, for the tested AL 5052 honeycombs, it can be said that inclined loads decrease the load bearing capacity significantly. The effect of bending moment on the cell walls becoming more significant than buckling loads with increasing loading angles could be the reason behind this. In general for all honeycombs the same sigmoid trend can be safely predicted for variation of crush stress, peak stress, and modulus with increasing loading angle. The young's modulus values at  $83^\circ$  and  $87^\circ$  are outliers for the predicted trend. This is attributed to the sample height misalignment, which is seen in the elastic region of the stress-strain curves for all the skewed samples. It is to be noted that height misalignment was not seen in the honeycomb sample with normal cell axes. .

## CHAPTER V

### 5. Conclusions and Future recommendations

#### 5.1. Properties of defect free (Wound) MG Honeycombs

1. The continuous ribbon winding manufacturing method has increased the strength of Metallic Glass Honeycombs by 40%.
2. Typical Honeycomb characteristics along the  $X_2$  direction were stronger than  $X_1$  with  $X_3$  being the strongest.
3. With this level of quality, Metallic Glass Honeycombs are 20% stronger than an aluminum honeycomb of even a 25% higher relative density.
4. Stiffer epoxies could improve the strength of Metallic glass honeycomb further.
5. The promise of MG honeycomb as an advanced structural material is conclusively proved.
6. Creating stronger adhesive bonds between rows and also at the nodes is speculated to increase the strength of MG Honeycombs by 20%.

## **5.2. Effect of Cell Axes Inclination or inclined loading on honeycomb strength**

1. Honeycomb strength decreases with cell axes inclination or with inclined loading angle.
2. A sigmoidal trend for decrease in strength and modulus of honeycombs with increase in loading angle is predicted.
3. Up to a transition loading angle, the drop in honeycomb strength is small.
4. Beyond the transition angle (typically  $72^\circ$ ) the drop in strength is significant.
5. The percentage decrease in strength and modulus with cell axes inclination or loading angle is material dependent.

Automating the manufacturing procedure for Metallic Glass Honeycombs would help achieve better geometry and structural consistency. The dynamic properties of MG Honeycombs have been investigated in a separate study [34] and higher peak and crush stresses was observed. Considering the negligible strain rate response of MG Honeycomb, an increase in crush strength of the honeycombs by at least 15-20% is speculated with automation of the manufacturing process. Using adhesives with better peel strength and stiffness would improve the properties of the honeycomb significantly. New adhesives suitable for foils are to be tested. Honeycombs of different densities have to be tested and compared to conclude the predicted sigmoidal trend. Finally, eliminating height misalignment by machining test sections out of unexpanded honeycombs would give a conclusive trend for variation of young's modulus.

## REFERENCES

- [1] B. Jayakumar, *et al.*, "Mechanical properties of amorphous metal honeycombs for ballistic applications," *ASME International Mechanical Engineering Congress*, 2009.
- [2] B. Jayakumar, "Metallic Glass Honeycomb and Composite Body Armor," Master's Thesis, Oklahoma State University, Stillwater, OK, 2009.
- [3] L. J. Gibson and M. F. Ashby, "Cellular solids : Structure & Properties," 2nd ed: Cambridge ;New York : Cambridge University Press, 1999., 1999, p. 528 p.
- [4] T. Wierzbicki, "Crushing analysis of metal honeycombs," *International Journal of Impact Engineering*, vol. 1, pp. 157-174, 1983.
- [5] A.-J. Wang and D. L. McDowell, "In-Plane Stiffness and Yield Strength of Periodic Metal Honeycombs," *Journal of Engineering Materials and Technology*, vol. 126, pp. 137-156, 2004.
- [6] H. N. G. Wadley, *et al.*, "Fabrication and structural performance of periodic cellular metal sandwich structures," *Composites Science and Technology*, vol. 63, pp. 2331-2343, 2003.
- [7] W. S. Burton and A. K. Noor, "Structural analysis of the adhesive bond in a honeycomb core sandwich panel," *Finite elements in analysis and design*, vol. 26, pp. 213-227, 1997.
- [8] U. o. Virginia. (03/16). <http://www.ipm.virginia.edu/newres/pcm.manuf/>.
- [9] A. J. Wang and D. L. McDowell, "Yield surfaces of various periodic metal honeycombs at intermediate relative density," *International Journal of Plasticity*, vol. 21, pp. 285-320, 2005.
- [10] J. Zhang and M. F. Ashby, "The out-of-plane properties of honeycombs," *International Journal of Mechanical Sciences*, vol. 34, pp. 475-489, 1992.
- [11] H. S. Lee, *et al.*, "Mechanical behavior and failure process during compressive and shear deformation of honeycomb composite at elevated temperatures," *Journal of Materials Science*, vol. 37, pp. 1265-1272, 2002.
- [12] M. J. Silva and L. J. Gibson, "The effects of non-periodic microstructure and defects on the compressive strength of two-dimensional cellular solids," *International Journal of Mechanical Sciences*, vol. 39, pp. 549-563, 1997.
- [13] S. D. Papka and S. Kyriakides, "In-plane compressive response and crushing of honeycomb," *Journal of the Mechanics and Physics of Solids*, vol. 42, pp. 1499-1532, 1994.
- [14] X. E. Guo and L. J. Gibson, "Behavior of intact and damaged honeycombs: A finite element study," *International Journal of Mechanical Sciences*, vol. 41, pp. 85-105, 1999.
- [15] O. Prakash, *et al.*, "A note on the deformation behaviour of two-dimensional model cellular structures," *Philosophical Magazine A*, vol. 73, pp. 739 - 751, 1996.
- [16] S. D. Papka and S. Kyriakides, "Biaxial crushing of honeycombs: --Part 1:

- Experiments," *International Journal of Solids and Structures*, vol. 36, pp. 4367-4396, 1999.
- [17] S. T. Hong, *et al.*, "Quasi-static crush behavior of aluminum honeycomb specimens under compression dominant combined loads," *International Journal of Plasticity*, vol. 22, pp. 73-109, 2006.
- [18] S.-T. Hong, *et al.*, "Dynamic crush behaviors of aluminum honeycomb specimens under compression dominant inclined loads," *International Journal of Plasticity*, vol. 24, pp. 89-117, 2008.
- [19] A. Petras and M. P. F. Sutcliffe, "Indentation failure analysis of sandwich beams," *Composite Structures*, vol. 50, pp. 311-318, 2000.
- [20] M. Doyoyo and D. Mohr, "Microstructural response of aluminum honeycomb to combined out-of-plane loading," *Mechanics of Materials*, vol. 35, pp. 865-876, 2003.
- [21] H. Kobayashi, *et al.*, "Dynamic and static compression tests for paper honeycomb core and absorbed energy," *Nippon Kikai Gakkai Ronbunshu, A Hen/Transactions of the Japan Society of Mechanical Engineers, Part A*, vol. 63, pp. 2580-2585, 1997.
- [22] J. J. Gilman, "Mechanical behavior of metallic glasses," *Journal of Applied Physics*, vol. 46, pp. 1625-1633, 1975.
- [23] A. Inoue, *et al.*, "Cobalt-based bulk glassy alloy with ultrahigh strength and soft magnetic properties," *Nat Mater*, vol. 2, pp. 661-663, 2003.
- [24] M. F. Ashby and A. L. Greer, "Metallic glasses as structural materials," *Scripta Materialia*, vol. 54, pp. 321-326, 2006.
- [25] A. L. Greer, "Metallic glasses...on the threshold," *Materials Today*, vol. 12, pp. 14-22, 2009.
- [26] M. Chen, *et al.*, "Extraordinary Plasticity of Ductile Bulk Metallic Glasses," *Physical Review Letters*, vol. 96, p. 245502, 2006.
- [27] A. H. Brothers and D. C. Dunand, "Porous and foamed amorphous metals," *Mrs Bulletin*, vol. 32, pp. 639-643, Aug 2007.
- [28] "US Patent 2010/054305."
- [29] A. R. Bhat, "Finite element modeling and dynamic impact response evaluation for ballistic applications," *MS Thesis, Oklahoma State University, USA*, 2009.
- [30] U. MetGlas Inc. (3/17). *About Metglas®*, Inc. Available: <http://www.metglas.com/about.htm>
- [31] U. MetGlas Inc. (2009, 03/17/2011). Magnetic Alloy 2826MB (nickel-based).
- [32] *PAMG-XR1 5052 Aluminum Honeycomb*, I. Plascore Data sheet 2011.
- [33] D. P. Melody, "Advances in room temperature curing adhesives and sealants—a review," *British Polymer Journal*, vol. 21, pp. 175-179, 1989.
- [34] A. Bhat, *et al.*, "Dynamic Compressive Behavior of Fe-based Amorphous Metal Honeycombs (under review)," in *TMS Annual Meeting and Exhibition (2011)*, San Diego, 2011.

## APPENDICES

### Appendix I

#### Design concepts for ribbon winding method of manufacturing Metallic Glass Honeycombs

##### Concept 1

A tear drop shape is a combination of a circle and a triangle. From this it was visualized that winding ribbons around pins would yield the tear drop geometry. A design for this using a base plate with holes, stud and tube was conceptualized (Figure AI - 1).

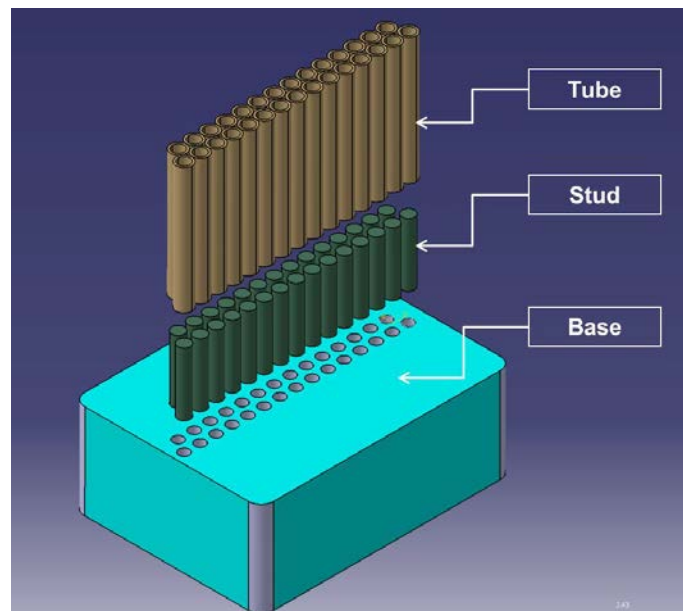


**Figure AI - 1 Base plate with threaded holes; Studs and pins.**

In this concept a metal block with threaded holes serves as the base. The hole diameter on the base plate is 1.5mm and the center-to-center spacing is 3.25 mm. Studs of size 1.5mm diameter are screwed on to the base plate. Tubes of internal diameter slightly

more than that of the stud and with an external diameter of 3.175 mm are inserted on to the studs. MG ribbon is wound around the tubes as explained in detail in (section 2.2)

The 3.25 mm center-center hole spacing takes into account the tube diameter, ribbon thickness, and tolerance ( $3.175\text{mm} + 0.06\text{mm} + \text{tolerance}$ ). The same result could be achieved using just base plate with holes and pins. However, the wall thickness of the holes on the base plate would be too thin to permit this design. This method provides very tight tolerances for hole diameter and center spacing, the cost of which did not justify the result achieved.

## Concept 2

Concept 2 is a variation of Concept 1 wherein to accommodate the diameter to center spacing limitations of the holes on the base plate tapered pins could be used. This allows for a required center distance of 3.235 mm with the diameter of the holes being half the center spacing.

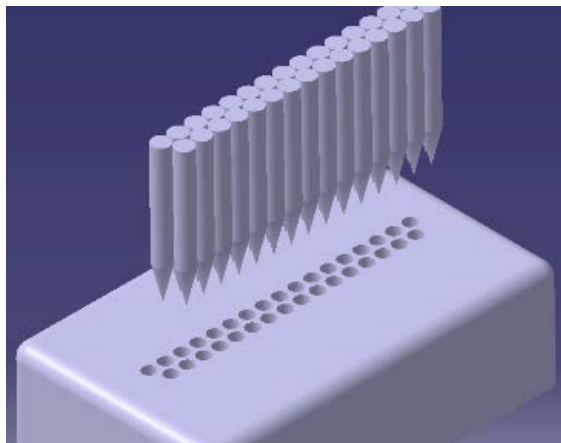


**Figure AI - 2 Base with small holes and pins with tapered ends.**

Highly precise spacing of holes was required and the pins had to be custom machined which increased the cost of the device.

Concept 3: Lab scale semi-automated method of manufacturing tear-drop lattice honeycombs

Concept 3 is an effort to automate the manufacturing process of tear-drop lattice up to the point of forming the geometry. Adhesive application was planned to be manual. It was named the Cell-Maker. A stepwise explanation of the concept is provided in the following paragraphs. Figure AI - 3 shows the main components of the cell maker: X-Blades, Y-Blades and Sliders.

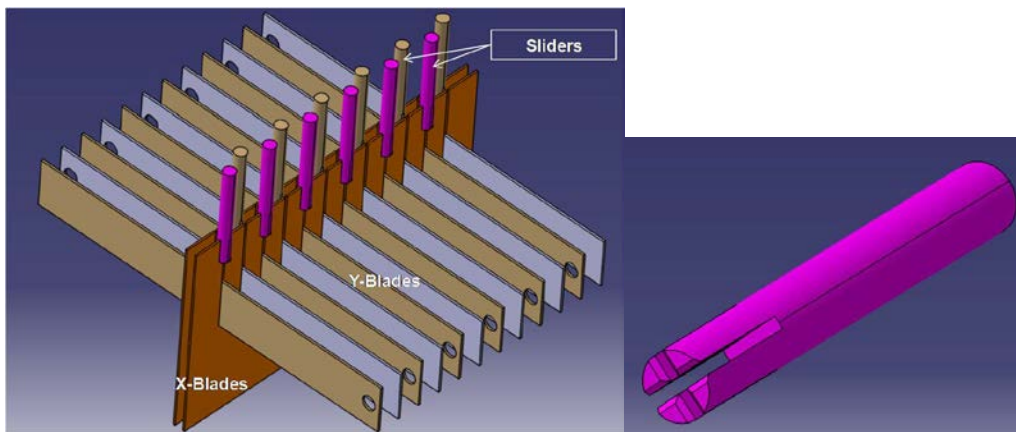


**Figure AI - 3 The main components of the Cellmaker.**

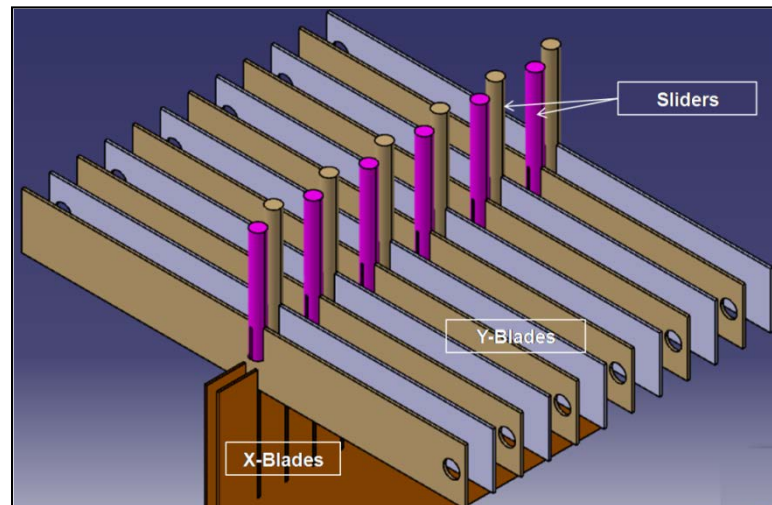
The kinematic constraints of the X-Blades, Y Blades and the slider are tabulated in Figure AI - 3.

**Table A1 - 1 Kinematics of Cell-maker's components**

	<b>X</b>	<b>Y</b>	<b>Z</b>
<b>X-Blades</b>	-	-	-
<b>Y-Blades</b>	-	Translation	Translation
<b>Sliders</b>	Translation	-	-

### ***Working mechanism of the Cellmaker***

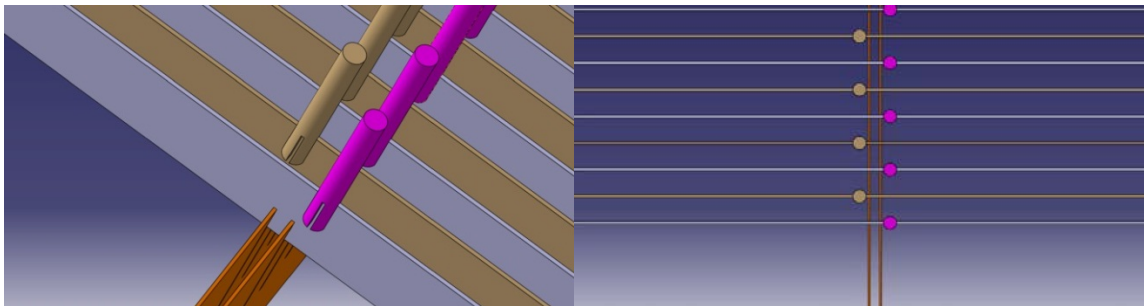
***Step 1*** From the initial position (Figure AI - 3), the Y Blades move up lifting the slider along the Z-axis as shown in Figure AI - 4.



**Figure AI - 4** Y-Blades have slid up lifting the Sliders along.

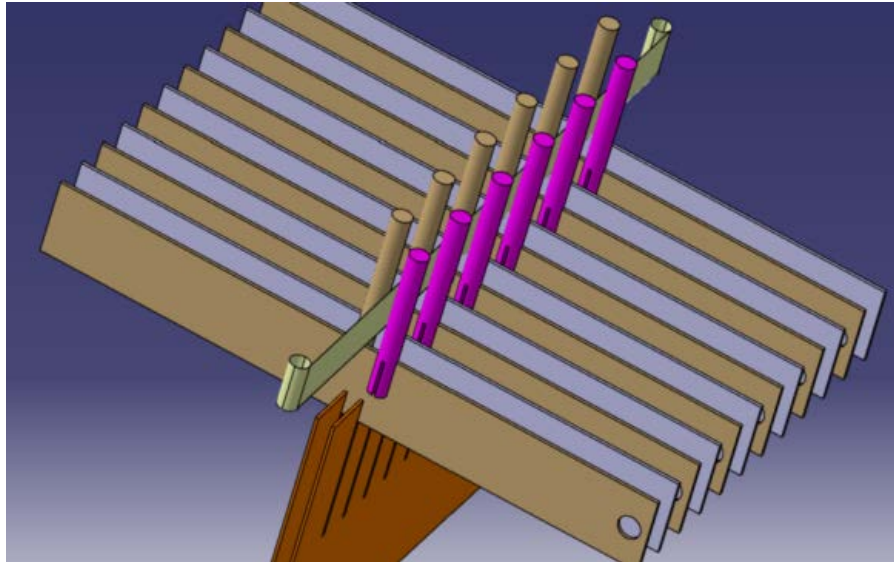
***Step 2*** The sliders move apart making way for the ribbon to be introduced between them.

Figure AI - 5 show a 3-D view and the top view of this step



**Figure AI - 5** A 3-D view and top view (right) of Step 2.

*Step 3* The ribbon is introduced in between the sliders



**Figure AI - 6 Ribbon introduced between the sliders.**

*Step 4* The sliders cross over weaving the Ribbon in a zig-zag manner. This is achieved by translating the Y-Blades using micrometer slides. The depiction shows that the sliders have moved or crossed over to the opposite sides

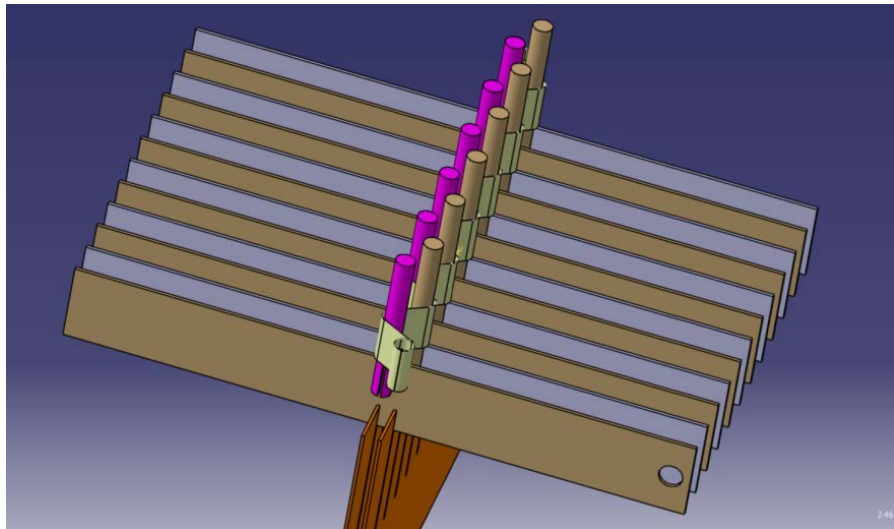


**Figure AI - 7 Ribbon wound in zig-zag manner.**

The Y-Blades move down bringing the sliders down. The sliders now are seated on the X blades (Figure AI - 8)

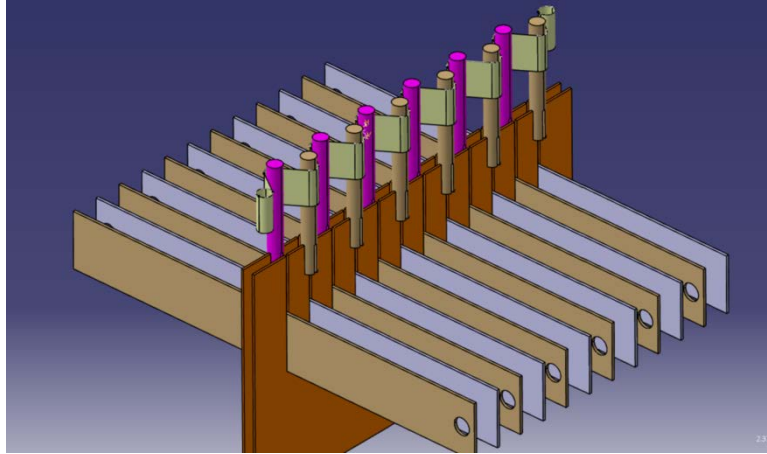


**Figure AI - 8 Y-Blades back to initial position.**

*Step 5* In this final step each slider is in tangential contact with its neighbors.

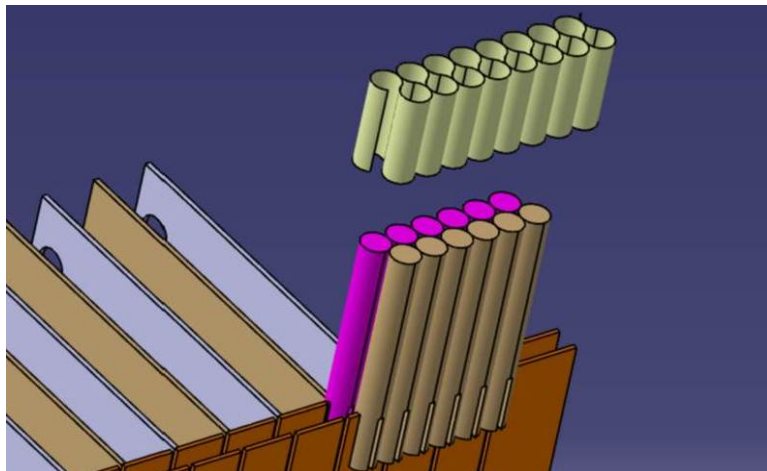


**Figure AI - 9 Sliders in tangential contact with neighboring sliders.**

The slots on the sliders and the blades required a very high precision machining for a snug-fit. The fit required here had to be conducive for a sliding motion while at the same time tight enough to keep the sliders from tipping. The size of the slider was 3.175mm and that of the slots was  $0.5 \pm 0.002$ . The application of adhesive between the nodes is manual and is carried out using a brush or an adhesive gun. Again the slot sizes on the sliders are extremely small as the slider diameter itself is 3.175mm. A rough cost benefit analysis made did not justify implementing this design.

## Appendix II

### Difficulties in machining expanded aluminum honeycombs

Aluminum 5052 honeycombs of thickness 12mm were machined on a band saw along carefully marked inclination lines to get skewed sections. But it was found that expanded aluminum honeycombs cannot be machined conventionally on a band saw along the  $X_1$  or  $X_2$  direction without deforming or crushing the cells. Figure AII-1 shows an Aluminum 5052 honeycomb sample crushed while trying to angular cuts on it along the  $X_1$  direction on a band saw.

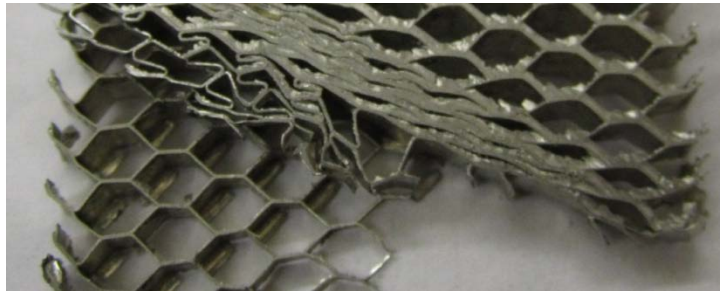


**Figure AII-1 Aluminum 5052 honeycombs crushed along the  $X_1$  direction while machining on a band saw.**

Cutting using a diamond saw is feasible, but not practical for large samples. An angular cut made using a diamond saw on a thin section is shown in Figure AII - 2.



**Figure AII - 2 Inclined cut made using a diamond edged saw on Al 5052 honeycombs.**

Complex machining methods like EDM are unsuitable due to the non-conductivity of the adhesive layer at the cell wall boundaries. Due to the machining

limitations imposed a practical way to cut expanded Aluminum honeycombs along the  $X_1$  and  $X_2$  directions, a cutoff saw was used to make honeycombs samples with an inclined cell axis.

VITA

Ganapathi Ranjan Mahadevan

Candidate for the Degree of

Master of Science

Thesis: CHARACTERIZATION AND ELIMINATION OF DEFECTS IN METALLIC  
GLASS HONEYCOMBS

Major Field: Mechanical and Aerospace Engineering

Biographical:

Born on the 31st of May year 1984 in Bangalore, India; Son of Mr. Mahadevan Ganapathi and Mrs. Lakshmi Mahadevan

Education:

Completed the requirements for the Master of Science in Mechanical and Aerospace Engineering at Oklahoma State University, Stillwater, Oklahoma in May 2011

Received Bachelor of Engineering Degree in Mechanical Engineering at Visveswaraiah Technological University, Belgaum, Karnataka/India in June 2006.

Experience:

Two years of professional work experience in Engineering design and CAD.

Graduate Research Assistant from May 2009-June 2011

Graduate Teaching assistant from August 2008-June 2009

Professional Memberships: ASME

Name: Ganapathi Ranjan Mahadevan

Date of Degree: July, 2011\*

Institution: Oklahoma State University

Location: Stillwater, Oklahoma

Title of Study: CHARACTERIZATION AND ELIMINATION OF DEFECTS IN  
METALLIC GLASS HONEYCOMBS

Pages in Study: 54

Candidate for the Degree of Master of Science

Major Field: Mechanical and Aerospace Engineering

### Abstract

This work focuses on quantification and elimination of defects in the new class of amorphous metallic glass honeycombs (MGH) developed in 2009. A new lab scale method of manufacturing was devised to produce defect free MGH, and it has reduced cell wall misorientation from  $15^\circ$  to  $1.5^\circ$  and also yielded a more uniform cell geometry. A threefold improvement in the strength of MGH was observed with the use of this new manufacturing method. MG Honeycombs have exhibited 20% higher crush strength and 20% higher peak strength than Al honeycombs of higher relative density.

The effect of cell axis misorientation on honeycomb strength related to the effect of inclined loads on honeycomb strength was studied using skewed aluminum honeycomb sections with different cell axis inclinations. A sigmoidal decrease in the strength of honeycombs with increasing loading angles was found. This research gives insight into the potential of Metallic Glass Honeycombs as structural materials. It also suggests the advantages expected for more precise automated mass production of the new material. Further, it helps in understanding the effect of inclined loads on honeycomb performance.

ADVISER'S APPROVAL: Jay C Hanan

---